USGS
science for a changing world

Postglacial Lahars and Potential Hazards in the White Salmon River System on the Southwest Flank of Mount Adams, Washington

Bulletin 2161

U.S. Department of the Interior
U.S. Geological Survey

Availability of Publications of the U.S. Geological Survey

Order U.S. Geological Survey (USGS) publications by calling the toll-free telephone number 1-888-ASK-USGS or contacting the offices listed below. Detailed ordering instructions, along with prices of the last offerings, are given in the current-year issues of the catalog "New Publications of the U.S. Geological Survey."

Books, Maps, and Other Publications

By Mail

Books, maps, and other publications are available by mail from—

USGS Information Services
Box 25286, Federal Center
Denver, CO 80225

Publications include Professional Papers, Bulletins, Water-Supply Papers, Techniques of Water-Resources Investigations, Circulars, Fact Sheets, publications of general interest, single copies of permanent USGS catalogs, and topographic and thematic maps.

Over the Counter

Books, maps, and other publications of the U.S. Geological Survey are available over the counter at the following USGS Earth Science Information Centers (ESIC's), all of which are authorized agents of the Superintendent of Documents:

- Anchorage, Alaska–Rm. 101, 4230 University Dr.
- Denver, Colorado–Bldg. 810, Federal Center
- Menlo Park, California–Rm. 3128, Bldg. 3, 345 Middlefield Rd.
- Reston, Virginia–Rm. 1C402, USGS National Center, 12201 Sunrise Valley Dr.
- Salt Lake City, Utah–2222 West, 2300 South
- Spokane, Washington–Rm. 135, U.S. Post Office Building, 904 West Riverside Ave.
- Washington, D.C.–Rm. 2650, Main Interior Bldg., 18th and C Sts., NW.

Maps only may be purchased over the counter at the following USGS office:

- Rolla, Missouri–1400 Independence Rd.

Electronically

Some USGS publications, including the catalog "New Publications of the U.S. Geological Survey" are also available electronically on the USGS's World Wide Web home page at **http://www.usgs.gov**

Preliminary Determination of Epicenters

Subscriptions to the periodical "Preliminary Determination of Epicenters" can be obtained only from the Superintendent of Documents. Check or money order must be payable to the Superintendent of Documents. Order by mail from—

Superintendent of Documents
Government Printing Office
Washington, DC 20402

Information Periodicals

Many Information Periodicals products are available through the systems or formats listed below:

Printed Products

Printed copies of the Minerals Yearbook and the Mineral Commodity Summaries can be ordered from the Superintendent of Documents, Government Printing Office (address above). Printed copies of Metal Industry Indicators and Mineral Industry Surveys can be ordered from the Center for Disease Control and Prevention, National Institute for Occupational Safety and Health, Pittsburgh Research Center, P.O. Box 18070, Pittsburgh, PA 15236–0070.

Mines FaxBack: Return fax service

1. Use the touch-tone handset attached to your fax machine's telephone jack. (ISDN [digital] telephones cannot be used with fax machines.)
2. Dial (703) 648–4999.
3. Listen to the menu options and punch in the number of your selection, using the touch-tone telephone.
4. After completing your selection, press the start button on your fax machine.

CD-ROM

A disc containing chapters of the Minerals Yearbook (1993–95), the Mineral Commodity Summaries (1995–97), a statistical compendium (1970–90), and other publications is updated three times a year and sold by the Superintendent of Documents, Government Printing Office (address above).

World Wide Web

Minerals information is available electronically at **http://minerals.er.usgs.gov/minerals/**

Subscription to the catalog "New Publications of the U.S. Geological Survey"

Those wishing to be placed on a free subscription list for the catalog "New Publications of the U.S. Geological Survey" should write to—

U.S. Geological Survey
903 National Center
Reston, VA 20192

Postglacial Lahars and Potential Hazards in the White Salmon River System on the Southwest Flank of Mount Adams, Washington

By James W. Vallance

U.S. GEOLOGICAL SURVEY BULLETIN 2161

UNITED STATES DEPARTMENT OF THE INTERIOR
BRUCE BABBITT, Secretary

U.S. GEOLOGICAL SURVEY
Charles G. Groat, Director

Reston, Virginia 1999

For sale by
U.S. Geological Survey
Information Services
Box 25286
Denver, Colorado 80225-0286

LIBRARY OF CONTRESS CATALOGING IN PUBLICATION DATA

Vallance, J.W.,
Postglacial lahars and potential hazards in the White Salmon River system on the southwest flank of Mount Adams, Washington / by James W. Vallance.
p. cm. — (U.S. Geological Survey bulletin ; 2161)
Includes bibliographical references and index.
Supt. of Docs. no.: I 19.3:2161
1. Lahars—Washington (State)—Adams, Mount, Region.
2. Volcanichazard analysis—Washington (State)—Adams, Mount, Region.
3. Geology—Washington (State)—Adams, Mount, Region.
I.Title. II. Series
QE75.B9 no. 2161
[QE599.U5]
557.3 s–dc21 97-14535
[551.3'07'0979755] CIP
ISBN.0-607-88066

COVER: *Mount Adams from the south. Holocene lahar surface of the Trout Lake lowland in the foreground.*

CONTENTS

PLATES

[Plates are in pocket]

FIGURES

TABLES

Graphic design and manuscript preparation by
Christine Janda, U.S. Geological Survey, Cascades Volcano Observatory, Vancouver, Washington

Postglacial Lahars and Potential Hazards in the White Salmon River System on the Southwest Flank of Mount Adams, Washington

By James W. Vallance

ABSTRACT

Mount Adams, a stratovolcano in southwestern Washington State, formed during Pleistocene time and reached roughly its present size before the end of the Fraser glaciation, which occurred between 25,000 and 12,000 years ago. Since the last glaciation, Mount Adams has erupted at least nine times, producing eight peripheral lava flows and a cinder cone at the summit but no pyroclastic flows. No stratigraphic evidence was found for the occurrence of lahars concurrently with eruptions; in fact, at least one lahar and one debris avalanche occurred during apparently dormant intervals.

At least five lahars and a debris avalanche, originating at Mount Adams, moved into the White Salmon River drainage basin during the past 12,000 years. The deposits produced by these lahars range in volume from 4 to 66 million cubic meters and they moved as much as 60 kilometers down the valley. About 6,000 years ago, the largest of the lahars inundated about 15 square kilometers of the lowland near Trout Lake and dammed a tributary stream to form Trout Lake. About 200 years ago, another lahar filled valleys to depths as much as 50 meters, and produced run-ups of as much as 30 meters on objects in its path, but left only thin veneers on valley sides and floors. Three smaller lahars and the debris avalanche of 1921 extend between 5 and 15 kilometers from Mount Adams.

The two largest lahars and the debris avalanche began as slope failures of hydrothermally altered rock from the cirque that forms the accumulation zone of the White Salmon and Avalanche Glaciers. Rocks in the headwall of the cirque, as well as in the deposits of the avalanche and lahars, contain the following distinctive secondary minerals: alunite, kaolinite, smectite, and opal. The hydrothermal alteration that formed these minerals weakened the volcanic structure, thereby setting the stage for slope failure. Formation of the secondary minerals, especially smectite and kaolinite, reduced permeability and increased porosity, thereby increasing the capability of the rocks to retain moisture. The slide masses that formed the two lahars apparently contained enough moisture to move as wet flows.

Exposures of altered andesite on the southwest, east, and north sides of Mount Adams indicate that hydrothermal alteration has variably affected at least 4.3 square kilometers of the central cone. Alteration in rocks that form the summit plateau is most severe, and alteration of rocks that form the flanks extends at least 1,000 meters below the summit; this indicates a volume of 1.5 to 3 billion cubic meters of altered rock near the summit of the volcano. This altered rock is a potential source of lahars and debris avalanches as large or larger than any of postglacial age at Mount Adams.

If future events at Mount Adams are similar in scale and type to those of postglacial time, the hazard from lahars or debris avalanches greatly exceeds that from lava flows and pyroclastic flows. Lahars, especially those resulting from slope failures of large volume, are dangerous because of their ability to move great distances downstream at speeds of tens of kilometers per hour. Beyond the slopes of the volcano, lahars are most dangerous along valley floors. If future magmatic eruptions are like those of the past, they will probably occur at vents on the flanks of the volcano and produce cinder cones and lava flows. Lava flows would probably

extend no more than about 15 kilometers from their sources. Fallout of cinders from cinder cones could extend from several kilometers to tens of kilometers downwind. Eruptions producing pyroclastic flows, if they occur, are likely to produce tephra fallout for several tens of kilometers downwind. Because Mount Adams is situated in wilderness surrounded by National Forest and an Indian Reservation, flank eruptions are unlikely to endanger nearby communities. An eruption at or near the summit of Mount Adams, however, could rapidly melt snow and ice, causing floods and lahars to sweep far down valleys.

If Mount Adams becomes active, State and local officials need to collaborate with scientists in planning how to cope with an eruption. Such a plan might include restricting public access to potentially hazardous areas, establishing evacuation plans for areas likely to be threatened, and installing lahar- and flood-warning devices in endangered valleys. A network of seismic, geodetic, and visual monitoring needs to be established as quickly as possible in order to determine the possible nature and extent of hazards.

INTRODUCTION

Mount Adams is a large stratovolcano in southwestern Washington State about 50 km (kilometers) north of the Columbia River and 50 km east of Mount St. Helens (fig. 1). The glacier-covered cone of andesitic lava and breccia towers 2,500 m (meters) above the surrounding Cascade Range. The present cone was formed before the last major glaciation, which occurred between 25,000 and 12,000 years ago (Porter and others, 1983). The lowermost lava flows exposed in the main cone have an age of about 460,000 years B.P. (before present) and overlap the eroded remnants, which range in age from 460,000 to 520,000 years B.P., of an older andesitic center called the Hellroaring volcano (Hildreth and Lanphere, 1994).

Although the volcano, as it appears today, was almost entirely constructed prior to the last glaciation, several hazardous events have occurred since glacial time. Such events included flank eruptions, which produced lava flows and cinder cones, and debris avalanches and lahars that moved many kilometers down valleys. Lahars are the most common and most hazardous volcanic processes at Mount Adams.

Purpose and Scope

This report describes the results of a study assessing volcanic hazards at Mount Adams Volcano. If a volcano behaves in the future as it has in the past, knowledge of its past behavior may be used to assess potential hazards. Although Mount Adams has not erupted during historic time, the nature of its past activity can be inferred by studying deposits of prehistoric events. The purpose of this study was to examine the physical characteristics, distribution, place of origin, and manner of emplacement of postglacial volcanic deposits, particularly lahars, on the southwest flank of Mount Adams for the purpose of assessing potential hazards. This study of lahars was limited to the southwest side of the volcano, because other sides of the volcano are sparsely populated.

Sections of this report include pertinent geography, terminology, regional geology, and a summary of volcanism at Mount Adams. In the main body of the report are: (1) documentation of the process and extent of hydrothermal alteration at Mount Adams, (2) descriptions of lahar and debris avalanche deposits on the southwest side of Mount Adams, and (3) assessment of volcanic hazards at Mount Adams.

Drainage

The White Salmon and Avalanche Glaciers, which cut deeply into the southwest flank of Mount Adams, form the headwaters of the White Salmon River, a southerly flowing tributary of the Columbia River (fig. 1). On other sides of Mount Adams the Lewis, Cispus, and Klickitat Rivers drain radially west, northwest, and southeast.

The White Salmon River catchment here is divided into four reaches: (1) the upper catchment, (2) the upper narrows, (3) the Trout Lake lowland, and (4) the lower narrows. The upper catchment, a reach deeply eroded by Pleistocene glaciers, begins at timberline (an elevation of about 1,950 m), and ends down valley at an elevation of about 900 m. The upper catchment of the White Salmon River includes: the upper White Salmon River valley, the Salt Creek-Cascade Creek valley (fig. 2), and the Morrison Creek valley. At an elevation of 900 m, the White Salmon River enters the upper narrows (fig. 1), a 300- to 400-m-wide gorge that has a steep gradient (28 m/km). The gorge is carved in andesitic and basaltic lava flows. Below the upper

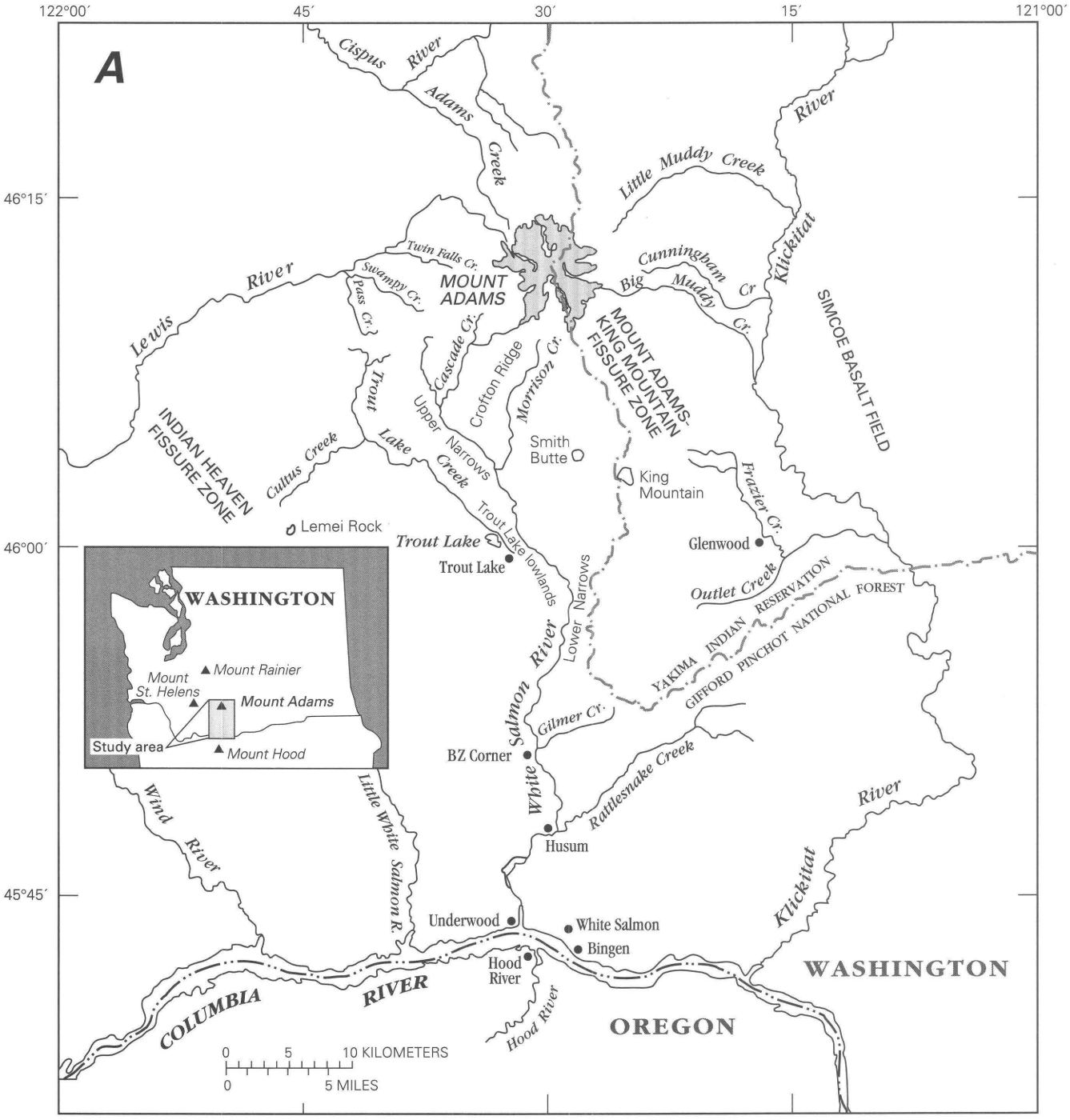

Figure 1A. The study area includes the southwest flank of Mount Adams and the White Salmon River basin.

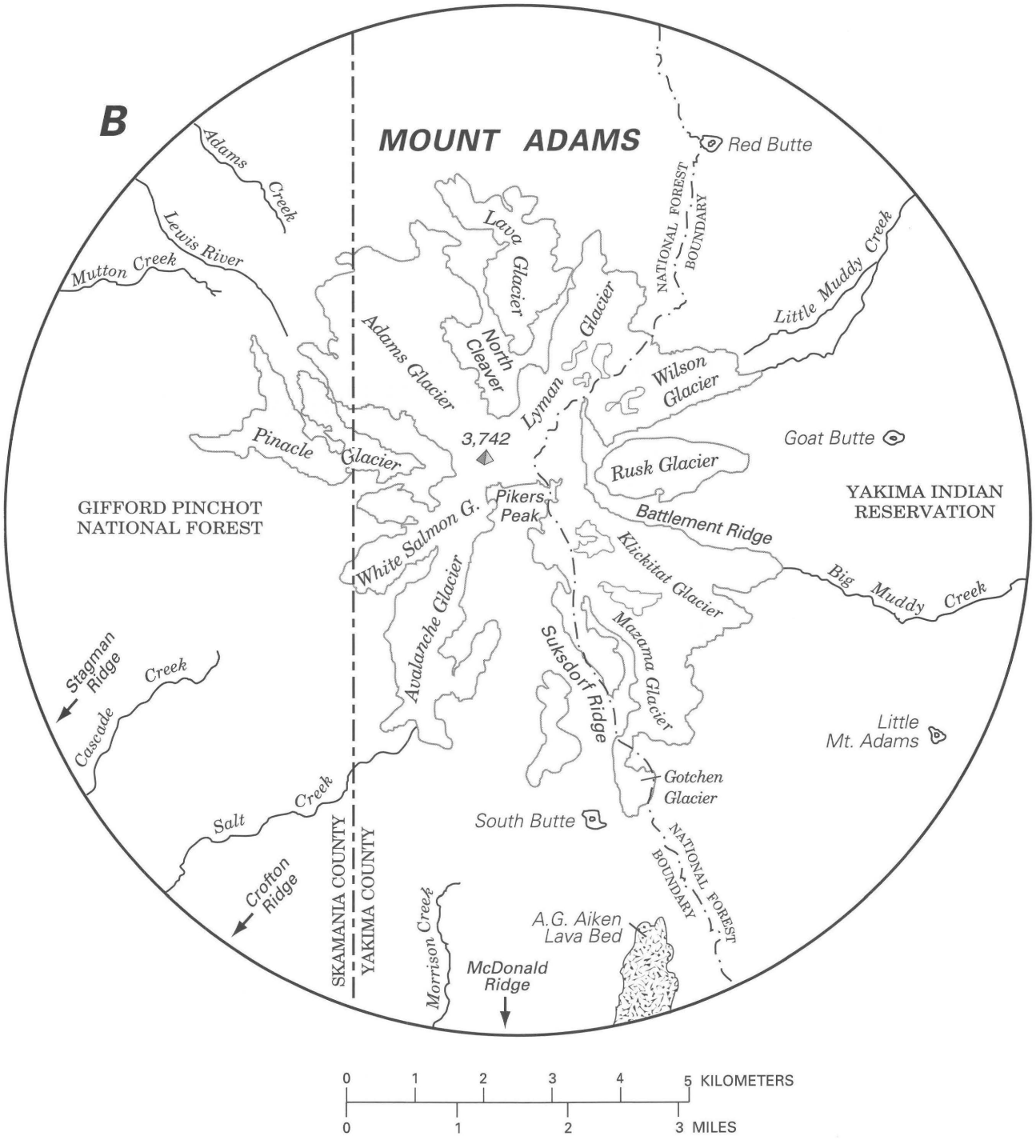

Figure 1*B*. Detailed enlargement of study area.

narrows, the White Salmon River enters the Trout Lake lowland (fig. 1), a broad flat valley that has a width of 2 to 5 km and an average gradient of 7.5 m/km. Here, the White Salmon River is joined by Trout Lake Creek. A Holocene lahar that descended the White Salmon River dammed the creek to form a small lake named Trout Lake. The lowland is underlain by a Pleistocene lava flow and by Holocene lahars. Because the lahar deposits are more fertile than are the surrounding lavas, a small community has grown in the Trout Lake lowland. Further downstream, at an elevation of 500 m, the White Salmon River incises Pleistocene valley-flow basalt and older lavas that underlie the White Salmon River valley. Typically, this gorge, here named the lower narrows of the White Salmon River (fig. 1), is 100 to 400 m wide and 20 to 50 m deep. The White Salmon River emerges from the gorge at Husum and flows 11 km in a confined valley to its confluence with the Columbia River.

Terminology

The word "lahar" is an Indonesian word for volcanic debris transported by water (van Bemmelen, 1949, p. 191). The term is used here to refer to a rapid flow of volcanic debris and water, or to deposits resulting from such flowage; this definition is consistent with the usage of Crandell (1971), Fisher and Schmincke (1984), and Scott (1988). Debris flow is a term used to indicate any flowing mixture of debris and water having sediment concentration greater than 60 percent by volume or 80 percent by weight. Flows having higher water contents, so high that they possess fluvial characteristics, yet carry very high sediment loads, are termed hyperconcentrated flows; depth-integrated sediment concentrations between 20 and 60 volume percent or 40 and 80 weight percent characterize such flows (Beverage and Clubertson, 1964). Some debris flows may transform

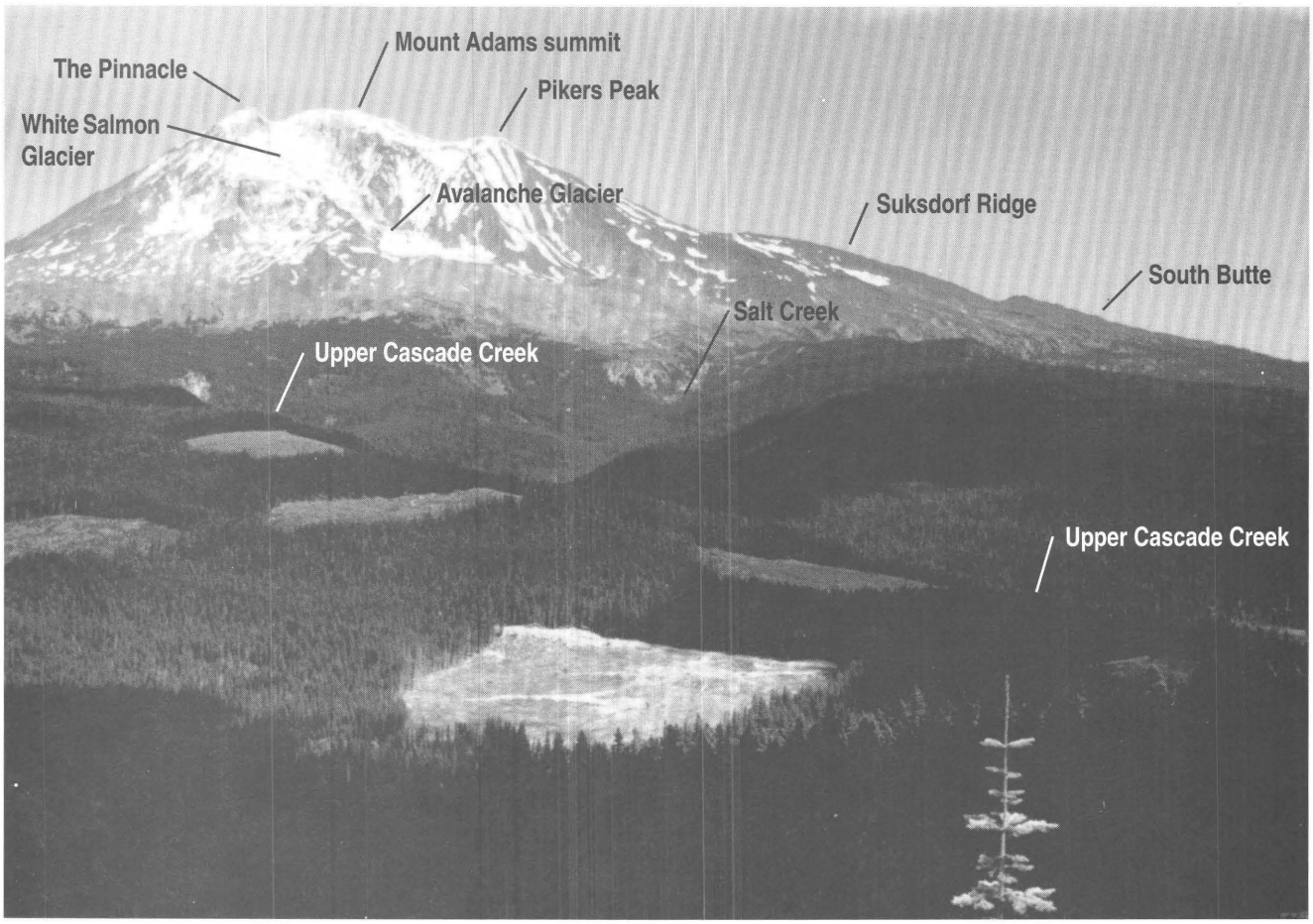

Figure 2. The southwest side of Mount Adams, showing the summit of Mount Adams, the Pinnacle, Pikers Peak, Suksdorf Ridge, South Butte, White Salmon and Avalanche Glaciers, and Cascade and Salt Creeks.

downstream to hyperconcentrated flows as they overtake and incorporate river water and thus become more dilute (Janda and others, 1981; Pierson and Scott, 1985; and Scott, 1988). Deposits of hyperconcentrated flow may be best distinguished from those of debris flows by their better sorting (Scott, 1988). Mudflow, in the sense of a debris flow having a greater than 50 percent sand, silt, and clay solid fraction (Crandell, 1971; Varnes, 1978), is not used in this report except in the informal name, Trout Lake mudflow of Hopkins (1976). However, the term mudflow is used as a synonym for debris flow.

A more significant criterion for distinguishing among debris flows is the clay content. In this report, cohesive and noncohesive debris flows are distinguished by the ratio of clay to total sand, silt, and clay. Vallance and Scott (in press) showed that a ratio of 0.05 or greater for cohesive debris flows is consistent with sediment-size data from lahars at Mount Rainier and Mount St. Helens. Noncohesive debris flows have less clay. The basic distinction between the terms, however, is the differentiation between noncohesive flows, which transform downstream to more dilute types and cohesive flows, which remain debris flows to their termini.

Sources of water in lahars include water that is within debris prior to movement and water that mixes with debris to form lahars. Avalanching volcanic rocks, especially those that have been affected by hydrothermal alteration, commonly contain sufficient moisture before movement to form lahars when the avalanching debris dilates and begins to flow (Schuster and Crandell, 1984). Water formed when hot rock flows over snow and ice is commonly incorporated into lahars. Similarly, the breaching of a crater lake will provide ample water to form lahars. Heavy rains, which mobilize unconsolidated debris may provide water for lahars.

Slope failures at volcanoes produce mass movements that move initially as debris avalanches but may later grade into flows of more complex behavior. Debris avalanche is a term that connotes sudden, rapid flowage of wet or dry, incoherent, unsorted mixtures of rock and soil in response to gravity (Schuster and Crandell, 1984). In this report the term debris avalanche also implies that the debris was unsaturated at the time of deposition. Some debris avalanches grade into cohesive lahars; others dewater after deposition, producing lahars that may extend beyond their distal margins.

In volcanic terrain, debris avalanches have commonly been described as lahars (Siebert, 1984), and some deposits of debris avalanches and lahars are difficult to differentiate. However, large debris avalanches (those with volumes of 1 km^3 or greater) exhibit readily identifiable features. These features include hills, mounds, longitudinal or transverse ridges, and occasional closed depressions (Glicken, 1982; 1986). Some hills and mounds include huge, commonly shattered blocks of rock ranging in size from tens to hundreds of meters in maximum dimension as well as blocks of coherent but unconsolidated deposits of similar size. Other hills are formed by lithologically heterogeneous blocks, some of which are parts of continuous stratigraphic successions and probably were transported by the avalanche in the same stratigraphic sequence that they had within the volcano (Crandell and others, 1984). At Mount Adams, where mass movements are rather small (5 million to 100 million m^3), debris avalanche features are subtle. Debris avalanches at Mount Adams display small mounds, but not hills, ridges, and closed depressions. Short runouts and irregular surfaces typically characterize small debris avalanches seen at Mount Adams; long runouts and flat profiles best characterize lahars. In lowland areas cohesive lahars commonly are normally graded.

Avalanches of swiftly moving, hot rock debris produced by eruptions are called pyroclastic flows and form pyroclastic flow deposits. Although pyroclastic flow deposits are present at Mount Adams (Hildreth and others, 1983), none of postglacial age are known. When an airborne plume of ash and lapilli accompanies a volcanic eruption, the ash and lapilli fall out downwind as tephra. The term tephra is used here to refer to wind-transported pyroclastic ash and lapilli, or to deposits of such fragments.

Geology of the Mount Adams Area

The bedrock in the Mount Adams area is composed entirely of volcanic and volcaniclastic rocks. On the southwest side of Mount Adams, the principal Tertiary units are the Ohanapecosh Formation, the Grande Ronde Basalt, and the Wanapum Basalt (fig. 3*A*). The Eocene Ohanapecosh Formation, which crops out near Trout Lake and in Trout Lake Creek valley, includes interbedded lavas and volcaniclastic rocks (Hammond, 1980). The Grande Ronde and Wanapum Basalts are formations of the Miocene (about 16.5 to 12 million years ago (m.y.a.)) Yakima Basalt Subgroup of the

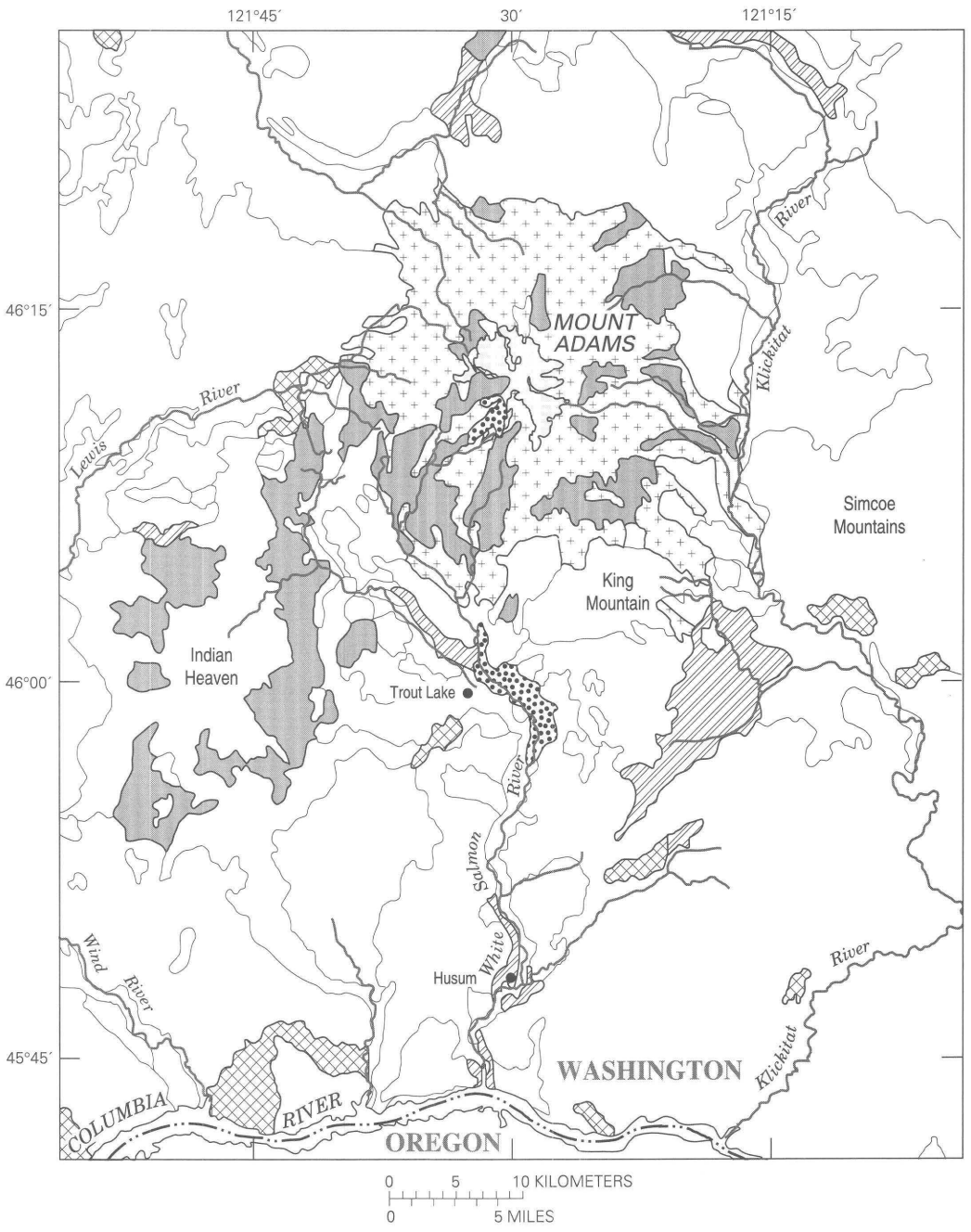

Figure 3*A*. Upper Pleistocene sediments and andesite, dacite, and basalt of the Mount Adams study area. Geology adapted from Smith (1993).

Columbia River Basalt Group of tholeiitic flood basalts; these formations crop out extensively in the lower White Salmon River drainage (fig. 3*C*).

Mount Adams is located near the center of an area of widespread Quaternary volcanism (fig. 3*B*). The Mount Adams volcanic field (Hildreth and Lanphere, 1994; Hildreth and others, 1983) merges with the coeval Indian Heaven volcanic field (Hammond and others, 1976) to the west and overlaps the other Simcoe Mountains volcanic field (Sheppard, 1967) to the east. Mount Adams itself is situated among a group of more than 60 discrete vents which trend from north-northwest to south-southeast and form the Mount Adams volcanic field (Hildreth and Lanphere, 1994; Hildreth and Fierstein, 1995).

Most units of the Indian Heaven volcanic field are west of the study area; but one, gray, phyric, olivine-plagioclase basalt called Basalt of Ice Cave, now underlies 30 km of the White Salmon River valley between Trout Lake and Husum (fig. 3*B*) (Hammond, 1980). Basalt of Ice Cave originated at Lemei Rock, partially filled the ancient White Salmon River valley and produced a flattened stretch, which the White Salmon River has only partially incised (Hammond and others, 1976; 1977). The basalt overlies a soil along the White Salmon River gorge that has a radiocarbon age of 22,100 ± 300 B.P. (Hildreth and Fierstein, 1995) and lies between drift of the last two major glaciations.

Of the numerous Pleistocene lavas that crop out in the Mount Adams volcanic field north and south of Mount Adams, most are basalt, but a few are andesite or dacite (Hildreth and Fierstein, 1995). Several of these units, all between about 600,000 and 200,000 years old, crop out along the upper narrows of the White Salmon River. Between 120,000 and 100,000 years B.P., voluminous pahoehoe basalts erupted from King Mountain fissure zone south of Mount Adams (fig. 3*B*) (Hildreth and Lanphere, 1994). Olivine basalt, erupted from several vents south of Mount Adams makes up basalt of Smith Butte (fig.3*B*), which has a potassium-argon age of 14,000 ± 13,000 years B.P. (Hildreth and Lanphere, 1994) and intertongues drift of the last two major glaciations (Hopkins, 1976).

Glaciation

The ability to recognize glacial deposits from three Quaternary advances is necessary to differentiate them from lahar and debris avalanche deposits and to constrain the ages of volcanic deposits. Hopkins (1976) defined three informal units of glacial deposits at Mount Adams. These are, from oldest to youngest, the White Salmon drift, the McDonald Ridge drift, and the Big Muddy Creek drift. The interval following the last major Pleistocene glaciation is generally known as postglacial time.

Hopkins (1976) suggested that his White Salmon drift was equivalent to the Hayden Creek Drift of Mount Rainier (Crandell, 1969; Crandell and Miller, 1974). The White Salmon drift crops out northeast of the Trout Lake lowland and in Trout Lake Creek valley. Deposits in the unit are unstratified, unsorted mixtures of pebbles, cobbles, and boulders in a matrix of sand, silt, and clay. Clasts are composed of andesite, olivine basalt, and aphyric or sparsely plagioclase phyric basalt that is typical of the Yakima Basalt Subgroup. Soil of the White Salmon drift is characterized by clay formation in the B horizon. The B horizon typically extends as deep as 2 to 3 m; weathering rind thicknesses on fine-grained basalts are 1 to 2 mm (Hopkins, 1976). Deposits of White Salmon drift, which are commonly overlain by yellowish-brown loess, lack distinct morphology, suggesting that they are ground moraine.

The McDonald Ridge drift of Hopkins (1976) was deposited during the Fraser glaciation between 25,000 and 12,000 years ago (Porter and others, 1983). Deposits are characterized by a yellowish-brown zone of weathering to a depth of approximately 1 m (fig. 4). Clasts of andesite, and locally of olivine and aphyric basalt in this zone are generally unweathered; weathering rind thicknesses vary from 0 to 0.5 mm. Within the study area, lateral and end moraines are well defined at elevations between 900 and 1,400 m. Moraines of McDonald Ridge age form five separate, concentric loops in the Morrison Creek valley (Hopkins, 1976); however, in other valleys, only one distinct moraine loop is apparent. The outer morainal loop on the southwest flank of Mount Adams is equivalent to the Evans Creek Drift of Crandell (1969) and Crandell and Miller (1974) at Mount Rainier.

On the east side of Mount Adams, neoglacial moraines of the Klickitat River catchment, ranging in age from about AD 1400 to the present, are designated as drift of Big Muddy Creek (Hopkins, 1976). Moraines of neoglacial age on the southwest flank of Mount Adams have not been studied. One or two moraine loops are apparent beyond the margins of the Avalanche and

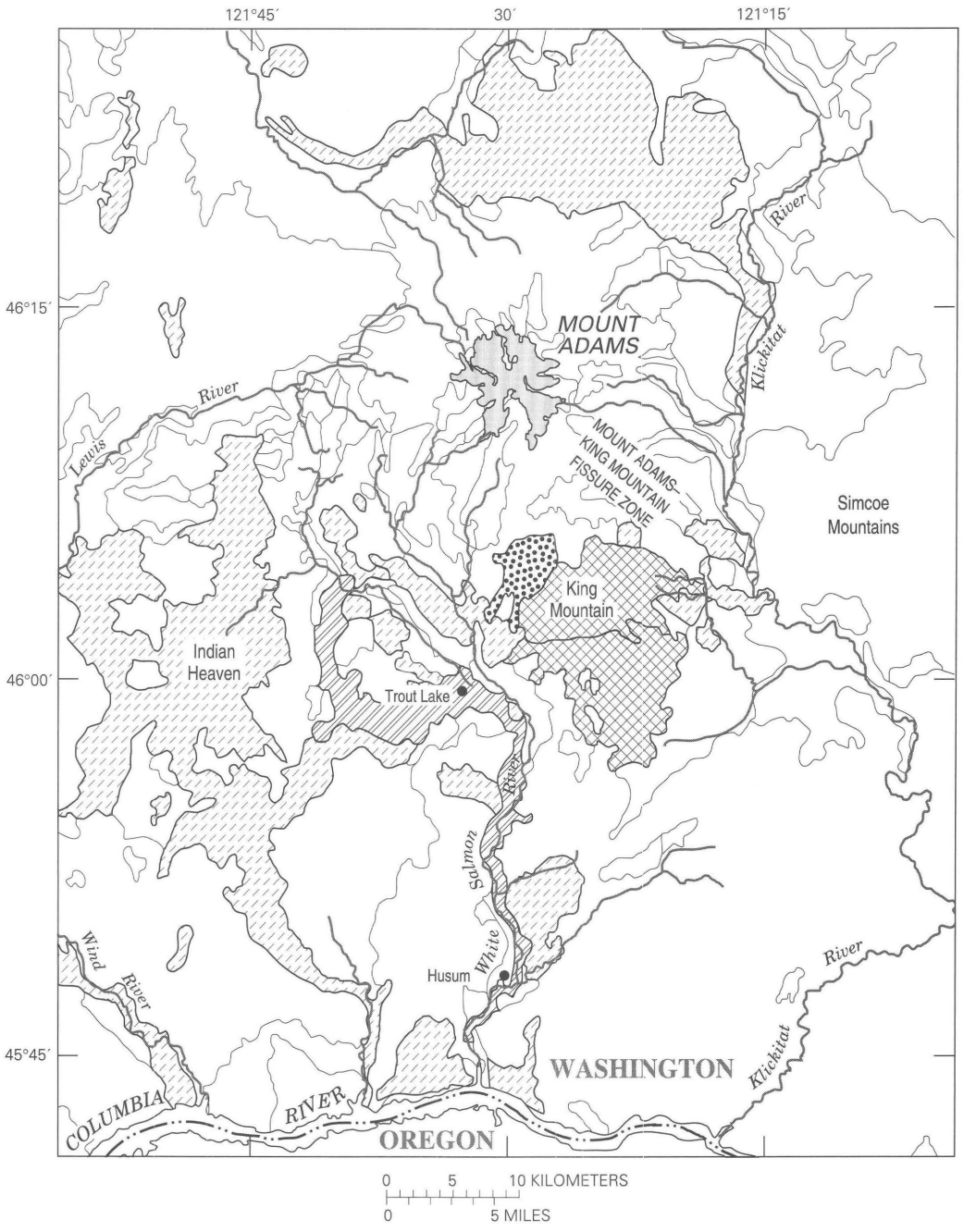

Figure 3*B*. Quaternary basalt lavas of the Mount Adams study area. Geology adapted from Smith (1993) and Hildreth and Fierstein (1995).

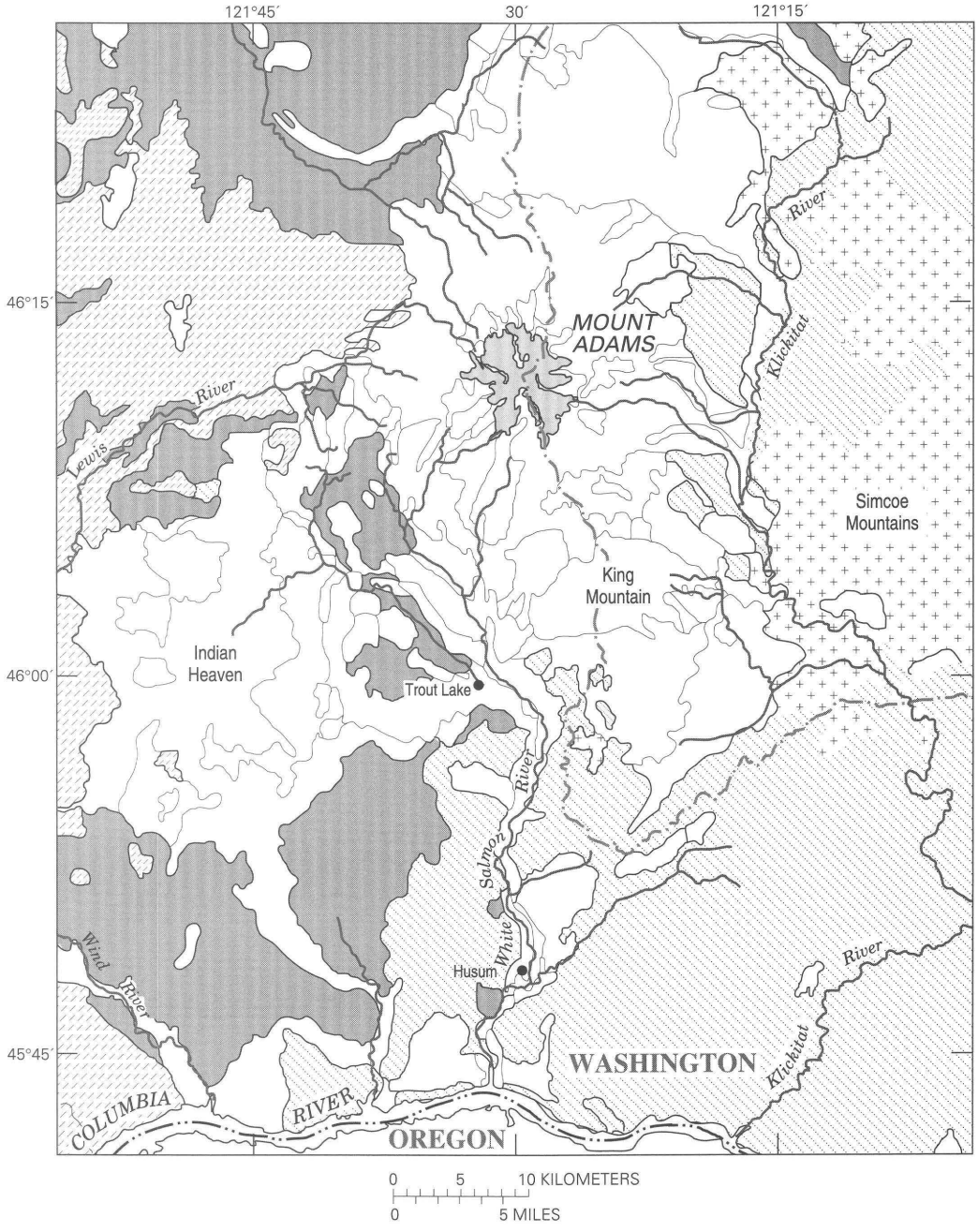

Figure 3C. Tertiary rocks of the Mount Adams study area. Geology adapted from Smith (1993).

White Salmon Glaciers. These moraines, which are sharply crested and sparsely vegetated, resemble 19th and 20th century moraines studied by Hopkins (1976) in the Klickitat valley.

Tephra

Tephra layers are useful as stratigraphic markers because they are widespread, distinct in outcrop, and amenable to dating; in this report they are used to constrain the ages of lava flows, lahars, and debris avalanches. Individual tephra layers result from single volcanic events; tephra sets are groups of tephra layers having similar ferromagnesian phenocryst assemblages (Mullineaux and others, 1972).

Seven widespread tephra units are identifiable south and west of Mount Adams, none of which came from that volcano. One unit originated from the prehistoric Mount Mazama in southern Oregon and the remaining six from eruptions of Mount St. Helens. These tephra layers are usually light colored, fine grained, and not more than several centimeters thick.

The characteristics, distribution, and age of tephra deposits from Mount St. Helens have been described by Mullineaux and others (1972, 1975), Crandell and Mullineaux, (1973), Mullineaux and others (1978), and Mullineaux (1986). The characteristics, distribution, and age of the Mazama ash has been given by Powers and Wilcox (1964) and Bacon (1983). Mullineaux, Crandell, and their coworkers have adopted upper case letters of the alphabet to name tephra units, and this convention is followed here.

Tephras identified at Mount Adams are set C, set J, set Y, set P, set W, and a layer erupted in 1980 from Mount St. Helens, and layer O from Mount Mazama. The characteristics and age of each tephra set are given

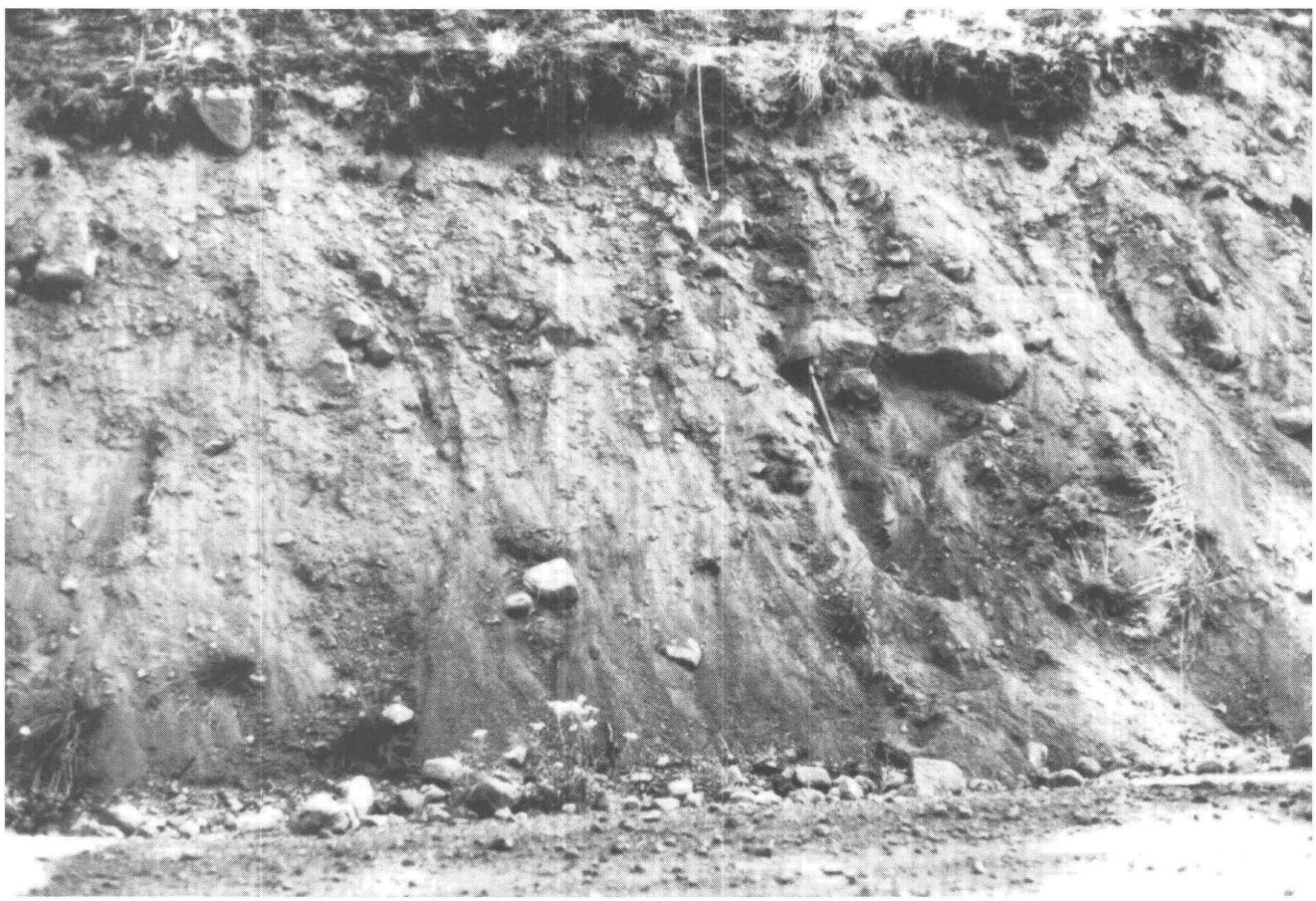

Figure 4. McDonald Ridge drift of Hopkins (1976) is equivalent to Evans Creek Crift of Fraser age (Crandell and Miller, 1974). The weathering zone (bracketed by tape measure) is about 80 cm thick. Shovel for scale.

Table 1. Characteristics useful for identification of tephra units
[Leaders (—) indicate no data]

Tephra unit age	Source volcano	Color	Average thickness (centimeters) South	Average thickness (centimeters) North	Grain size (centimeters)	Ferro-magnesian minerals[1]	Minimum refractive index for hypersthene[2]	Approxi-mate age (years)
1980	Mount St. Helens coarse ash	Light gray	Absent	1.0	Medium to	hy, hb	1.686-1.692	1980 A.D.
We	....do....	White	0-1.0	1.0-4.0	Coarse ash	hy, hb	1.705-1.710	1482 A.D.[3]
P	....do....	Light gray to brownish yellow	N/O[4]	5-10	Fine to coarse ash, lapilli to 0.5	hy, hb	1.688-1.694	2,500-3000
Y	....do....	Yellow to brownish yellow	N/O[4]	20-40	Coarse ash and lapilli to 2.0	cm, hb	----	3,400-4,000
O	Mount Mazama	Reddish yellow	3-7	3-7	Very fine ash	hy, hb, ag	1.684-1.689	6,800
J	Mount St. Helens	Very pale brown to yellowish brown	N/O[4]	([5])	Coarse ash and lapilli to 0.5	hy, hb	1,690-1,694	8,000-12,000
C	....do....	Yellow to brownish yellow	N/O[4]	([6])	Coarse ash and lapilli to 1.2	cm, hb, bt	----	36,000

[1] Hypersthene (hy), hornblende (hb), augite (ag), cummingtonite (cm), biotite (bt).
[2] Minerals were oriented with the spindle stage, then refractive indices were measured using the method of central focal masking.
[3] Tree-ring date (Yamaguchi, 1983).
[4] Not observed (N/O).
[5] Scattered lapilli and ash in a zone 20 cm thick.
[6] Scattered lapilli and ash in a zone 1.5 m thick.

in table 1. Each tephra was identified by its field characteristics, its stratigraphic position, and its ferromagnesian phenocryst assemblage. Refractive indices of hypersthene phenocrysts distinguish set W from other hypersthene-hornblende-bearing tephra layers, sets P and J.

Although no tephra layers from Mount Adams were observed in the study area, five tephra layers originating at Mount Adams overlie tephra layer Ye in a meadow 6 km southeast of the volcano (Hildreth and Fierstein, 1995). Four of the layers contain andesitic lithic-crystal ash and one contains andesitic, scoria as coarse as 2 cm. Three of the ash layers and the scoria layer also overlie tephra set P, but all underlie tephra layer We (Hildreth and Fierstein, 1995). The soutce vents of the tephra layers are unknown.

Volcanism at Mount Adams

Recent mapping (Hildreth and Fierstein, 1995) and high-resolution, potassium-argon dating (Hildreth and Lanphere, 1994) reveal that Mount Adams has been active nearly half a million years. The present cone is built on the eroded remnants of the older (about 500,000 to 520,000 years B.P.) Hellroaring volcano, centered about 5 km southeast of the modern summit. (Hildreth and Fierstein, 1995). Hildreth and his colleagues showed that the modern cone became active by about 460,000 years B.P. Hildreth and Lanphere (1994) suggest that activity at Mount Adams has been episodic and show that nearly all of the cone presently exposed above timberline was extruded during an eruptive spurt between 40,000 and 12,000 years ago.

The main cone of Mount Adams comprises breccia, scoria, and lava of porphyritic andesite to basaltic andesite that was erupted from several vents along a north-south trend (Hildreth and Fierstein, 1995). Hopkins (1969, 1976) recognized the compound structure of Mount Adams and suggested that the summit and Pikers Peak (south summit) are separate vents (fig. 2). The younger south cone (Pikers Peak) has coalesced with the main cone. Several other vents along

the ridge from Pikers Peak south to South Butte are sources of numerous andesite lava flows erupted during late Pleistocene time (Hildreth and Fierstein, 1995).

Mount Adams has been less active in postglacial time than it was in late Pleistocene time. Postglacial eruptions have produced only eight flank lava flows (plate 1; Hildreth and Fierstein, 1995). The only basaltic lava flow (Trappers Creek) is overlain by tephra set Y (3,500 years B.P.) and extends 13 km northeastward from its source, the scoria and spatter cone, Red Butte (plate 1). Andesite lava flows extending 8 to 10 km from their sources on the south (A.G. Aiken)(fig. 5) , north (Muddy Fork), and northwest (Takh Takh Meadows) are all overlain by tephra set Y (3.500 years B.P.) and underlain by tephra set O (6,800 years B.P.) (plate 1; Hildreth and Fierstein,1995). Andesitic lava flows on the northwest and east flanks of the volcano are also overlain by tephra set Y (Hildreth and Fierstein, 1995). Cunningham Creek lava flow extends about 15 km eastward from its source about 1 km east of Goat Butte (plate 1). Two other small andesitic lava flows high on the south and east flanks of Mount Adams (plate 1) are poorly constrained stratigraphically but are apparently of postglacial age (Hildreth and Fierstein, 1995).

Figure 5. The south side of Mount Adams. The A.G. Aiken lava bed, shown in the foreground, is typical of Holocene lava flows, which originate on the flanks of the volcano and extend 5 to 10 km down slope.

The morphology of a small cone at the summit of Mount Adams (fig. 6) suggests that it is much younger than the main cone. Hildreth and Lanphere (1994) report a potassium-argon age of 15,000±8,000 on this unit suggesting that it may have been formed during very late Pleistocene or Holocene time. This small cone has a well-defined, asymmetric crater whose northeast wall is incised by the summit ice cap. This andesitic cone is composed of vitrophyric, vesicular, rubbly lava, fragmental blocks, and subordinate scoria (Hildreth and Fierstein, 1995). Much of the rock of the summit cone is hydrothermally altered.

The five tephra units mentioned in the previous section are representative of the most recent eruptions at Mount Adams. Each of the tephra units is younger than 3,500 years B.P., but none of them is younger than 1482 A.D. None of these units is tied to a specific eruptive vent. Vents associated with the lavas high on south and east flanks of the volcano (plate 1) are the most likely sources (Hildreth and Fierstein, 1995).

HYDROTHERMAL ALTERATION

The main cone of Mount Adams is composed of a central core of fragmental andesite scoria and breccia that grades outward to radially dipping, alternating layers of breccia and massive andesite. The permeable clastic core and clastic beds of the outer slopes have permitted the upwelling of hydrothermal gases and the subsequent downward flow of acidic hydrothermal fluids that have variably affected the volcanic edifice. Exposures of solfatarized rock, presently visible in cliffs and cleavers of the east, north, and southwest flanks of the volcano, define a central, hydrothermally altered area of about 4.3 km^2, of which at least 0.55 km^2 has been moderately to severely altered (fig. 7). Permanent ice and snow conceal about 2.8 km^2 of the 4.3 km^2 hydrothermal area, but data from sulfur prospecting of

the 1930's suggests an additional 0.54 km^2 of extensively altered rock north of the summit in an area covered by up to 90 m of ice. Thus, at least 25 percent of the surface of the central cone is extensively altered. Cliffs and cleavers expose hydrothermally altered andesite more than 500, 800 and 1,000 m below the summit on the north, west, and east flanks of Mount Adams. These exposures indicate that hydrothermally altered andesite extends more than 1,000 m below the summit. If hydrothermally altered andesite is assumed to extend 500 to 1,000 m below the summit, 0.9 to 3.3 km^3 of Mount Adams' upper edifice is variably altered.

Between 1931 and 1935, Mr. Wade Dean's "Glacier Mining Company" mined solfatara deposits for sulfur in the gently sloping area north of the summit of Mount Adams. The summit crater is the center of the most intensive alteration; primary sulfur deposits occur there with gypsum, alum and silica. The alum $((Na,K)A1(SO_4)_2$ reported by Hodge (1934) and Fowler (1935) is mostly alunite $((K,Na)Al_3(SO_4)_2(OH)_6)$, possibly with a minor component of jarosite $(KFe_3(SO_4)_2(OH)_6)$. Fowler (1935) supervised sampling from eight test pits and sixteen drill holes north of the summit (locations shown in fig. 7). Samples from test pits contained between 11 percent and 79 percent sulfur by weight and samples from drilling sludge contained between 2 percent and 33 percent sulfur. Sulfur content generally decreased about 15 m below the surface. The sulfur was deposited under ice, at the ice-rock interface, near vents that emitted H_2S (Fowler, 1935).

Alunite, kaolinite, opal, and smectite are the most common mineral phases in altered andesite at Mount Adams. Elsewhere, replacement deposits containing these minerals commonly occur in concentric zones (Hall and Bauer, 1983). At Mount Baker, Frank (1983) suggested four such zones centered around vents of active fumaroles. In order of decreasing intensity these

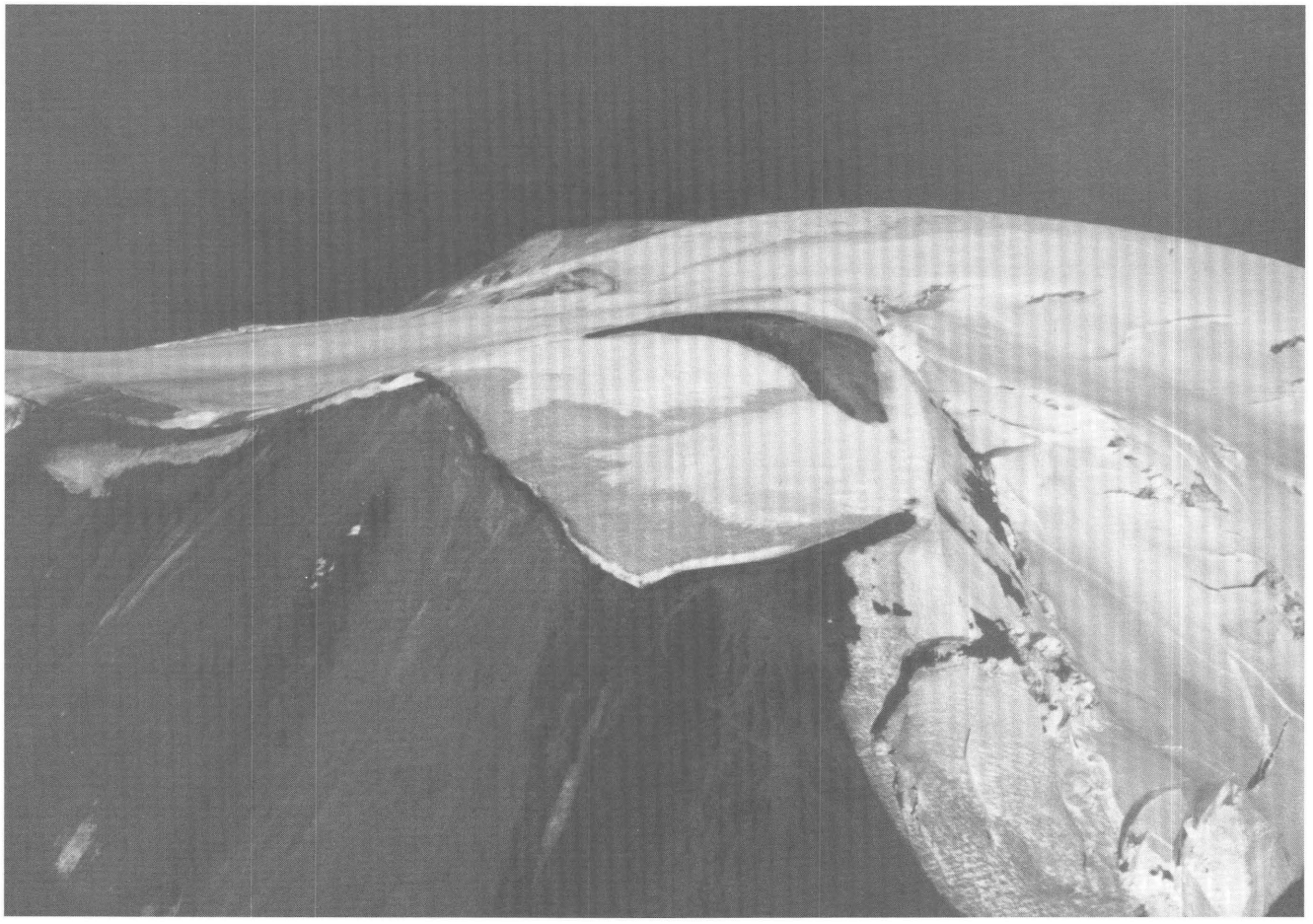

Figure 6. The view looking north toward the summit of Mount Adams. The summit cone in the foreground is much younger than the deeply dissected volcanic edifice in the background.

are: a central, silica-rich zone; an alunite-rich zone; a kaolinite-rich zone; and an outer, smectite-rich zone. The presence of such zones at Mount Adams is uncertain, but all four alteration products are present in avalanche debris in the White Salmon River drainage and in altered clasts from cliffs above Avalanche Glacier.

Alteration begins when ascending hydrogen sulfide gas is oxidized at or near the surface to form sulfuric acid:

$$H_2S + 2O_2 = H_2SO_4$$

Subsequently descending in the ground water, the sulfuric acid adds sulfate and hydrogen to surrounding rocks, removes soluble elements, and leaves behind aluminum and silica (a process known as acid sulfate leaching). Kaolinite and the silica phases, opal, cristobalite, and quartz, thus form from the alteration of plagioclase and volcanic glass (Hemley and Jones, 1964). In the presence of sulfuric acid, alunite may form by alteration of kaolinite (Hemley and others, 1969) or by precipitation from solution in veins (Frank, 1983). Incomplete leaching may result in residues of TiO_2 and $CaSO_4$. As hydrothermal waters are diluted, pH rises and sulfate becomes more soluble; in the presence of these less acidic hydrothermal fluids, smectite is favored over kaolinite and alunite (Frank, 1985).

Seven samples of hydrothermally altered debris were collected from an avalanche that descended the Avalanche Glacier in 1921. Both clay-sized and sand-sized fractions were analyzed by X-ray powder diffractometry. Minerals detected include: clay minerals, kaolinite, smectite, and a trace of chlorite; sulfate minerals such as alunite and possibly jarosite; traces of silica phases including opal and cristobalite; hematite; and unaltered minerals including plagioclase and a trace of augite (table 2). Comparison between clay-sized and sand-sized fractions suggests that smectite is more abundant in the clay-sized fraction, whereas hematite is more abundant in the sand-sized fraction.

XRD (X-ray diffraction) analysis of eight clast samples collected from debris on Avalanche Glacier indicated the presence of clay minerals such as kaolinite and smectite, sulfate minerals including alunite and gypsum, SiO_2 phases including opal and cristobalite, hematite, and plagioclase (fig. 8, table 3). In addition, Hildreth and others (1983) analyzed four samples from the area above the headwall of Avalanche Glacier which contained the secondary minerals, alunite, kaolinite, opal, cristobalite, quartz, and hematite; they also detected similar minerals in avalanche debris from the headwalls of the Adams, Wilson, Lyman, and Klickitat Glaciers (table 4). Comparing the data in tables 2 and 3 suggests that kaolinite is more abundant in clast samples than it is in clay- and sand-sized samples.

Phenocrystic hypersthene, augite, and plagioclase (ranging from andesite to labradorite), typify Mount Adams andesite. A few mafic rocks contain olivine (Hopkins, 1976; Hildreth and others, 1983), but none were observed. The andesites have porphyritic, pilotaxitic or hyalopilitic textures. On the main summit cone, glassy andesite increases with elevation (Fowler, 1935). Andesite of Mount Adams' main cone ranges from 57 percent to 62 percent SiO_2 (Hildreth and others, 1983).

Phenocryst phases of altered andesite tend to be opalized. Opal replaces plagioclase preferentially along more calcic zones (fig. 9); otherwise it replaces phenocryst phases along margins and fractures. Microprobe analyses of opalized phenocrysts indicate 85 percent to 90 percent SiO_2, traces of aluminum, and 8 percent to 15 percent water (total oxides are usually 85 to 92 percent; remainders are assumed to be H_20). Alunite may form in voids or fracture space created during opalization of the phenocrysts.

Lack of iron in microprobe analysis of altered magnetite grains indicate that iron is mobile, but that titanium contained in magnetite and in ilmenite exsolution lamelli is relatively immobile. The TiO_2 phase is probably anatase. A high SiO_2 concentration and a low refractive index suggest that opal is an important constituent of altered magnetite.

Microprobe analysis of fresh and altered groundmass shows leaching of mobile elements, magnesium, sodium, calcium and iron, and increasing hydration. Indices of refraction less than that of balsam suggest that opal is also a major component of the altered groundmass. Several microprobe analyses indicative of moderate aluminum content, as well as a lack of coarse-grained, aluminum-bearing minerals, suggest the presence of clay in the ground mass.

XRD traces show that kaolinite is a component of altered andesite, and moderate aluminum content in the analyses suggest that very fine-grained kaolinite may be abundant in the groundmass of some altered

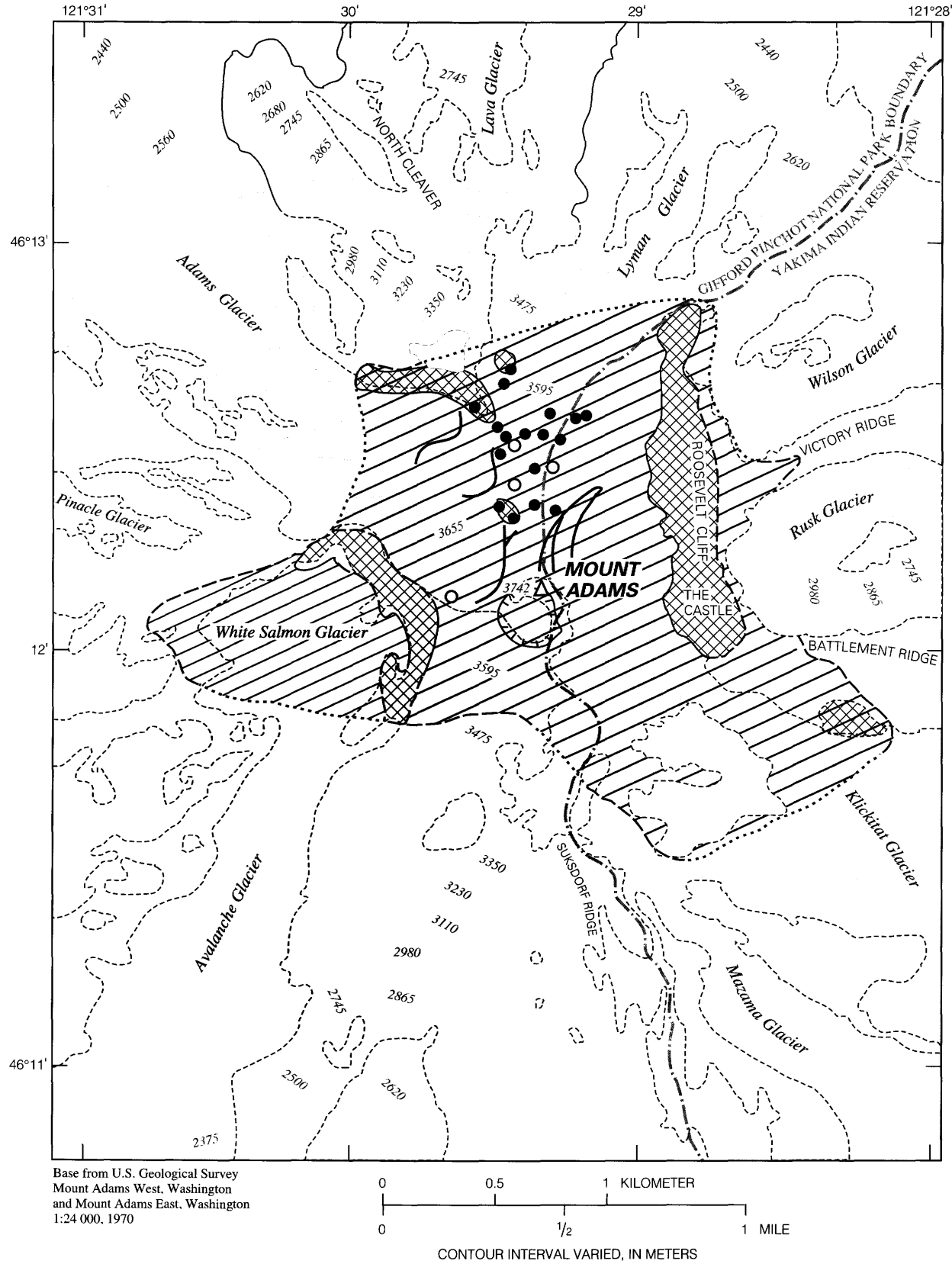

Figure 7. The summit area of Mount Adams. The lightly shaded area indicates the approximate extent of hydrothermal alteration based on aerial reconnaissance.

EXPLANATION

APPROXIMATE EXTENT OF HYDROTHERMAL ALTERATION

AREAS OF MORE SEVERE HYDROTHERMAL ALTERATION

CONTACT – Dashed where approximately located; dotted where concealed

TEST PITS AND DRILL HOLES INDICATING THE PRESENCE OF SULFUR – Approximately located (from Hodge, 1934, and Fowler, 1935)

TEST PITS AND DRILL HOLES INDICATING NO SAMPLE RETURNS – Approximately located

CRAVASSES WHERE SULFUR WAS DETECTED – Approximately located (Fowler, 1935)

CRATER RIM

GLACIERS

andesites. The original texture of the groundmass and phenocrysts is well preserved in most altered andesite (fig. 10). In some way, not clearly understood, hydrothermal action metasomatizes the original andesite without destroying original textures or changing volumes.

Alunite is the most common void-filling mineral. Other void-filling phases include kaolinite, smectite in some clasts, opal, chalcedony, and minor amounts of pyrite and hematite. Alunite occurs as pseudocubic rhombohedra, tabular laths with rhombohedral truncations, and anhedral granular masses; crystals range from clay- to silt-sized (fig. 11).

Altered andesites similar to those at the heads the glaciers on the north, east, and southwest sides of Mount Adams were the source of secondary minerals that were detected throughout debris avalanches which flowed down the flanks of the volcano. Similar minerals were detected in Holocene lahars that flowed many kilometers down the White Salmon River valley on the southwest flank. The hydrothermal minerals found in the lahars were formed in place in rocks at the head of the Salt Creek-Cascade Creek drainage before the lahars occurred. Hydrothermal alteration, which weakened the rocks, is the primary source of secondary minerals in the lahars. These and other lahars are the subject of the next section.

LAHARS IN THE WHITE SALMON RIVER DRAINAGE

Of seven lahars and a debris avalanche observed in the White Salmon River drainage, two predate and six postdate the Fraser glaciation. The oldest lahars, which probably came from Mount Hood, are included in this discussion for completeness; these lahars are important because they indicate that large, prehistoric lahars have crossed the Columbia River. The ages of two other lahars derived from Mount Adams are poorly constrained but may be early post glacial. Three lahars and a debris avalanche from Mount Adams were emplaced in the past 6,000 years. A new radiocarbon date and an older one (Hopkins, 1976) date the oldest of these lahars, the Trout Lake mudflow, to 5,200 years B.P. A younger lahar, bracketed by tephra sets P and W, was emplaced between 2,500 and 500 years B.P. Based on tree-ring counts and a radiocarbon date, the youngest lahar, the Salt Creek lahar, is slightly more than 200 years old. The debris avalanche occurred in May 1921.

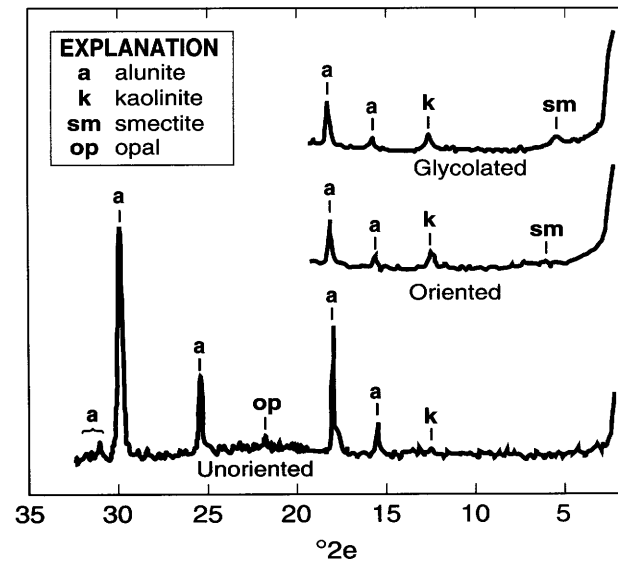

Figure 8. X-ray diffraction pattern of altered andesite sample, **MA 30**, showing alunite, kaolinite, smectite, and opal.

Table 2. Minerals detected by X-ray diffraction[1] in fine-grained, hydrothermally altered, avalanche debris collected in upper Salt Creek near Avalanche Glacier

Sample number	Sample description	Size fraction	Minerals identified[2]
MA 101	Yellowish-red (5YR 5/6)[3] pod containing clay- to granule-sized particles	sand clay	kaol/ht, sm/al, plag, aug kaol/sm/al, ht, plag, aug
MA 102	Very-pale-brown (10YR 8/3) lens containing clay- to granule-sized particles	sand clay	sm/kaol/plag?, al? sm/kaol/plag, aug
MA 103	Yellowish-brown (10YR 5/4) pod containing silt- to sand-sized particles	sand plag	sm//kaol, al, crist, opal
MA 104	Pale-yellow to gray (2.5Y 8/3 to 5Y 5/1) pod containing clay- to small-pebble-sized particles	sand clay	plag/sm/kaol, al, ag sm, plag//kaol, al
MA 105	Grayish-red-purple (7.5RP 4/3) pod containing clay- to granule-sized particles	sand clay	al, ht//kaol, plag al/ht, plag/sm, aug
MA 106	Light-gray (2.5Y 7/2) lens containing clay- to small-pebble-sized particles	sand clay	sm/plag/kaol, chl, al, aug sm/plag/chl, al?
MA 10	Light-gray (2.5Y 7/2) pod containing silt- to granule-sized particles	sand	sm/kaol, plag/al

[1] X-ray powder diffractometer with Copper K-alpha radiation was used. Oriented bulk mounts of each sample were prepared.

[2] Unaltered minerals: plag, plagioclase; aug, augite. Alteration minerals: sm, smectite, kaol, kaolinite; chl, chlorite; al, alunite; crist, cristobalite; opal, ht, hematite; jar, jarosite. Minerals are given in approximate order of abundance; slash denotes decrease in abundance; double slash denotes marked decrease in abundance.

[3] Munsell color notation.

Table 3. Minerals detected by X-ray diffraction[1] in samples of hydrothermally altered andesite collected from Avalanche Glacier. Oriented and unoriented mounts of the bulk sample were prepared

Sample number	Sample description	Minerals identified[2]	K:Na ratio in alunite[3]
MA 8	Medium-gray to brownish-gray and reddish-gray andesite--several zones present	plag/al/py bimodal	85:15, 45:55:
MA 10[4]	Fresh, medium-dark-gray, andesite with altered yellow and maroon encrustations	al, plag/kaol/opal, ht,sm	65:35
MA 11	Brownish-yellow, altered andesite	al/kaol/plag, opal?	65:35
MA 12[4]	Yellow to brownish-yellow, altered andesite	al/kaol/plag,opal	65:35
MA 30[4]	Light-yellowish-gray, altered andesite	al/kaol/sm,opal	60:40
MA 31[4]	Very-light-gray vein filling with altered andesite fragments	al//kaol,opal	70:30
MA 36[4]	Light-grayish-yellow, altered andesite	al,kaol/opal/crist	55:45
MA 50	White vein filling with gray altered andesite fragments	gyp/al/sm?	60:40

[1] X-ray powder diffractometer with Copper K-alpha radiation was used.

[2] Alteration minerals: al, alunite; kaol, kaolinite; sm, smectite; opal, crist, cristobalite; ht, hematite; gyp, gypsum; py, pyrite. Minerals are given in approximate order of abundance; slash denotes decrease in abundance; double slash denotes marked decrease in abundance.

[3] The position of the 102 (rhombohedral) major peak was used to estimate K:Na ratio after Cunningham and Hall (1976). The method of Parker (1962) suggests considerable scatter about these values.

[4] Both oriented and unoriented mounts of the sample were prepared.

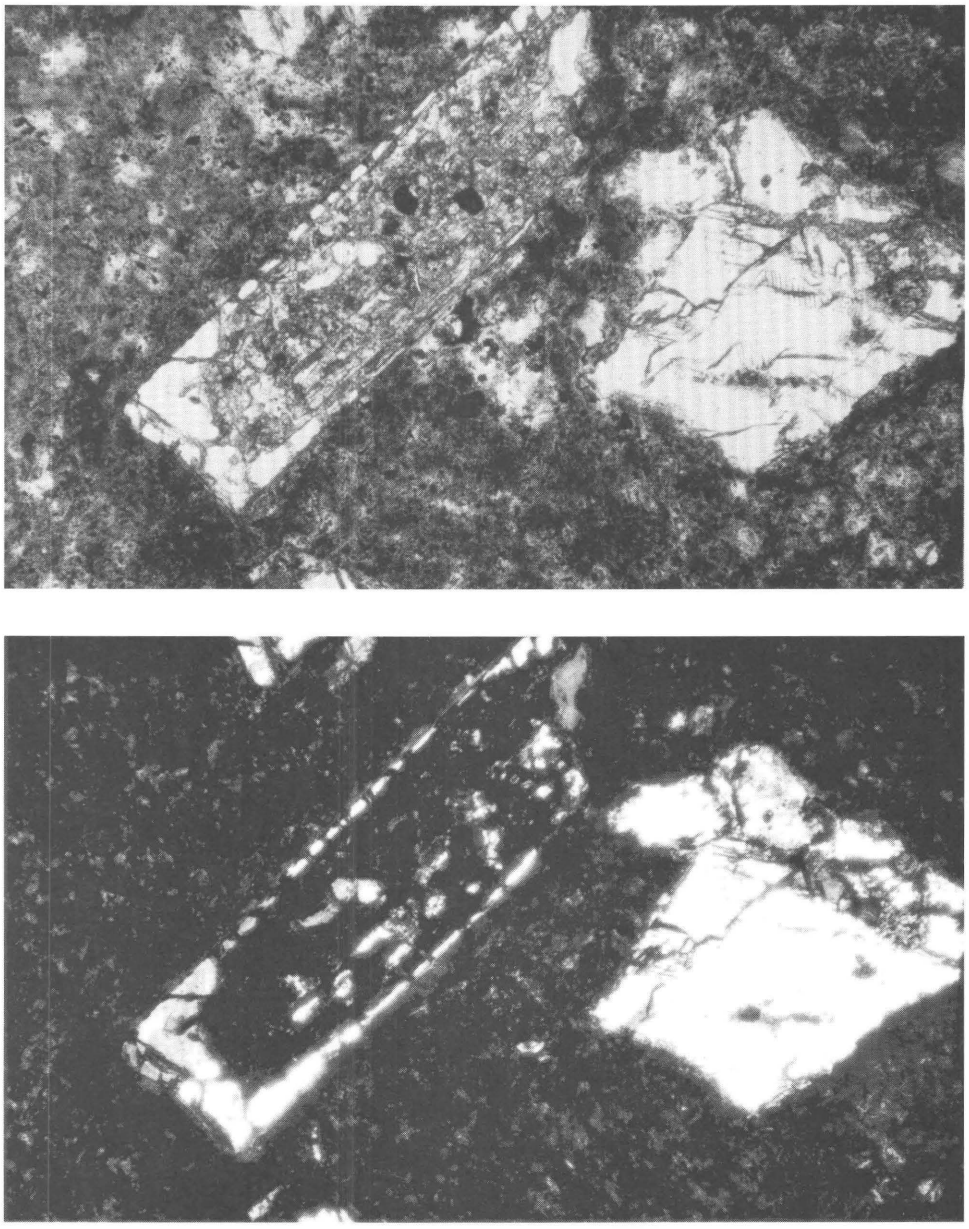

Figure 9. Photomicrographs (above, in plane light; below, in polarized light) of a partially altered plagioclase phenocryst. The more calcic core of the plagioclase has been preferentially opalized. The dimensions shown in the photomicrograph are 0.92 x 1.38 mm.

Table 4. Summary of minerals found in altered andesite by Hildreth and others (1983)

Part of mountain	Location	Number of samples	Minerals identified by XRD
SW	Top of cliffs above Avalanche and White Salmon Glaciers	4	Alunite, cristobalite, hematite, kaolinite, magnetite, opal, plagioclase, quartz
SW	Avalanches debris from headwalls of White Salmon and Avalanche Glacier	12	Alunite, cristobalite, geothite, gypsum, hematite, kaolinite, opal, plagioclase, smectite
S	Piker's Peak	1	Opal
E	Avalanche debris on Klickitat Glacier from its headwall	12	Alunite, gypsum, sulfur, kaolinite, smectite, opal, hematite
NE	Devils Garden avalanche debris from cleavers and headwalls above Lyman and Wilson Glaciers	4	Alunite, kaolinite, goethite hematite
N	Avalanche debris from headwall of Adams Glacier	21	Alunite, jarosite, pyrite, sulfur, kaolinite, smectite, opal,

Lahars near the Confluence with the Columbia River

The oldest lahars observed in the White Salmon River valley crop out on valley sides and terraces of the lower White Salmon River north of the Columbia River, and of the Hood River, south of the Columbia River (plate 2). The White Salmon River flows 70 km south from Mount Adams and the Hood River flows 50 km north from Mount Hood; both join the Columbia River nearly opposite one another. Because of this geographic coincidence it is not immediately apparent whether the lahars came from Mount Hood or from Mount Adams.

At the mouth of the White Salmon River, a lenticular lahar, 1 m thick, occurs within river gravel that is overlain by another 30-m-thick lahar. The same lahar assemblage also underlies terraces that are 100 m above the present valley floor along the lower Hood River valley. The assemblage includes one lahar that is 40 m thick, which here is informally called the Hood River lahar. This lahar, uppermost in the sequence, is correlative with the 30-m-thick lahar at the mouth of the White Salmon River. The lahar was identified no more than 4 km up the Hood River and 2 km up the White Salmon River valleys (plate 2).

A sequence of gravels and lahars is exceptionally well exposed in roadcuts along the west side of the White Salmon River valley between 0.3 and 0.5 km upstream from its confluence with the Columbia River. In one continuous roadcut, the stratigraphic sequence is (from bottom to top): cobble gravel; 2 m of boulder gravel of White Salmon River provenance; 50 cm of sand; a lenticular, sandy, pinkish-gray lahar; 5 m of cobble-to-boulder gravel of White Salmon River provenance; the 30-m-thick, pinkish-gray Hood River lahar; and fluvial sand and gravel of upper Columbia River provenance that is thought to be deposited by the last late Pleistocene scabland flood that washed down the Columbia River valley from eastern Washington.

Fragments of hornblende-pyroxene andesite are common within the matrix of both lahars and are abundant within transported blocks of pyroclastic-flow deposits scattered throughout the Hood River lahar. This rock type is apparently absent at Mount Adams (Hopkins, 1976; Hildreth and Fierstein, 1995; this study). It is, however, common at Mount Hood (Wise, 1969). Clast lithologies therefore suggest that Mount Hood, not Mount Adams, was the source of the lahars.

Evidence indicates that the Hood River lahar originated as a landslide on Mount Hood. Clay content averages 8 percent (table 5 , samples 26-28, fig. 12), and X-ray diffraction (XRD) patterns of the clay fraction demonstrate that plagioclase and smectite predominate (table 6). The presence of yellowish, altered andesite

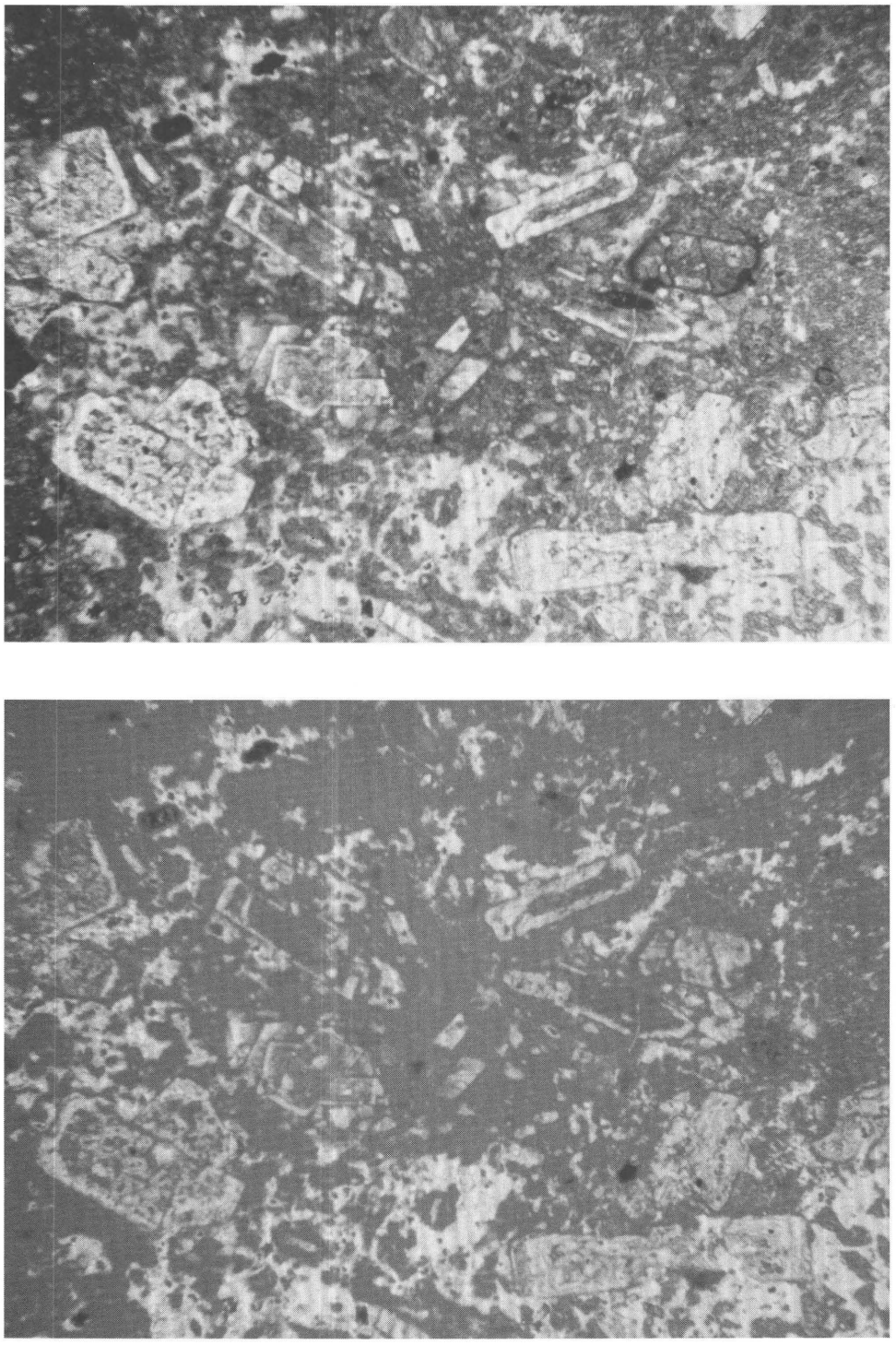

Figure 10. Photomicrographs (above, in plane light; below, in polarized light) of severely altered andesite showing preservation of the original texture of the andesite. The dimensions shown in the photomicrograph are 3.6 x 5.6 mm.

Table 5. Size-distribution data from samples of late Quaternary lahar, debris avalanche, and glacial deposits in the White Salmon River drainage
[Arranged from youngest at top to oldest at bottom]

Sample[1]	Location	Size distribution (percent by weight)					Median Phi diameter	Standard deviation
		gravel (>2.0mm)	sand (0.0625-2.0mm)	silt (0.004 - 0.625mm)	clay[2] (<0.004mm)	(<0.002mm)		
1.	1921 debris avalanche--Crofton Creek	49	36	8	7	5	-1.0	4.4
2.	Salt Creek lahar--upper Salt Creek	51	25	10	4	3	-1.1	5.0
3.	Salt Creek lahar--Crofton Creek	51	37	9	3	3	-1.1	4.6
4.	Salt Creek lahar--upper Cascade Creek	40	44	11	5	3	0.51	4.3
5.	Salt Creek lahar--Cascade Creek at Salt Creek	42	39	14	5	4	0.15	4.9
6.	Veneer, Salt Creek lahar--Cascade Creek at White Salmon River	42	51	5	2	2	-0.14	2.6
7.	Salt Creek lahar--Cascade Creek at White Salmon River	46	40	10	4	3	-1.1	4.3
8.	Salt Creek lahar--upper Trout Lake lowland	50	38	8	4	3	-1.1	4.5
9.	Weathering zone, Salt Creek lahar--Trout Lake lowland	57	32	9	3	2	-4.1	4.6
10.	Salt Creek lahar--Trout Lake lowland	68	23	6	2	2	-4.3	4.1
11.	Salt Creek lahar--Trout Lake lowland	73	19	6	2	2	-4.3	3.9
12.	Pre W post P lahar--upper Cascade Creek	57	35	5	3	2	-2.1	3.6
13.	"Hyperconcentrated" lahar--Cascade Creek at White Salmon River	47	50	2	1	0	-0.77	2.1
14.	Older lahar--Cascade Creek at White Salmon River	50	40	6	4	3	-1.0	3.2
15.	Trout Lake mudflow--upper Cascade Creek	48	36	11	5	4	-0.49	4.0
16.	Trout Lake mudflow--Cascade Creek	62	30	5	3	2	-2.9	3.9
17.	Trout Lake mudflow--upper Trout Lake lowland	61	25	8	6	5	-3.2	4.4
18.	Trout Lake mudflow--Trout Lake lowland at Trout Lake Creek	42	40	12	6	4	0.18	4.3
19.	Upper zone, Trout Lake mudflow--Trout Lake lowland at Trout Lake Creek	50	37	9	4	3	-1.1	4.3
20.	Lower zone Trout Lake mudflow--Trout Lake lowland at Trout Lake Creek	50	34	10	6	5	-1.2	4.7
21.	Trout Lake mudflow--Trout Lake	42	40	10	8	6	0.04	4.5
22.	Upper zone, Trout Lake mudflow--lower Trout Lake lowland	38	44	10	8	7	0.32	5.8
23.	Lower zone, Trout Lake mudflow--lower Trout Lake lowland	38	44	11	7	5	0.23	5.0
24.	Drift of Evans Creek age	43	43	11	3	2	-0.26	4.5
25.	Drift of Evans Creek age--weathering zone	40	45	13	2	1	0.51	4.1
26.	Large lahar near Columbia River	47	33	13	7	5	-0.26	5.1
27.	Large lahar near Columbia River	52	28	12	8	6	-1.3	5.1
28.	Large lahar near Columbia River	44	34	13	9	7	0.15	5.1
29.	Gray pod from large lahar near Columbia River	64	27	6	3	2	-2.7	4.1

[1] Samples in table 5 correspond with those in table 6.
[2] Note that clay (<0.004 mm) plus silt, sand, and gravel add to 100 percent while clay (<0.002 mm) plus sand, silt, and gravel do not add to 100 percent.

masses and of abundant smectite clay in the matrix indicate that this lahar contains abundant hydrothermally altered rock. At Mount Rainier lahars of Holocene age that contain high proportions of altered rock and secondary clay originated as avalanches derived from areas of hydrothermally altered rock (Crandell, 1971); the high proportion of altered rock in the Hood River lahar suggests that it had a similar origin.

Soil development on the uppermost lahar 2 km from the Columbia River along the the west side of the White Salmon River valley extends to a depth of 1.5 m and exhibits a prominent textural B horizon. Field criteria indicate that the clay content in the Bt horizon is greater than that in unweathered portions of the deposit and that its chroma is significantly higher (7.5YR 5/6; color according to Munsell color chart) than parent material (7.5YR 7/2). Clasts are partially decomposed in the weathered zone. This soil development resembles that described by Trimble (1963) for the upper Pleistocene Estacada Formation in the Portland area. That formation, which also contains lahars from Mount Hood, is weathered to a depth of 2 m and contains partially decomposed clasts in the zone of maximum weathering. A 14C date of sample W-5064, shows that the Hood River lahar is older than 38,000 years B.P. (table 7).

To have left such thick deposits on both sides of the Columbia River valley, the Hood River lahar must have temporarily filled that valley to a depth of at least 30 m. The emplacement of a lahar of similar volume today would have a catastrophic effect on the Hood River valley, and probably would cause flood surges that would affect low areas along the valley floor of the Columbia River far downstream from Hood River.

Lahars in Lower Cascade Creek

A sequence composed of a diamicton, a lahar, a crudely stratified lahar, and a lahar crop out along a stream cut in lower Cascade Creek (measured section 1). Lenses of sand and silt within the diamicton at the base of measured section 1 (unit 1) indicate that it is not a lahar; it is probably glacial drift. Lahars higher in the

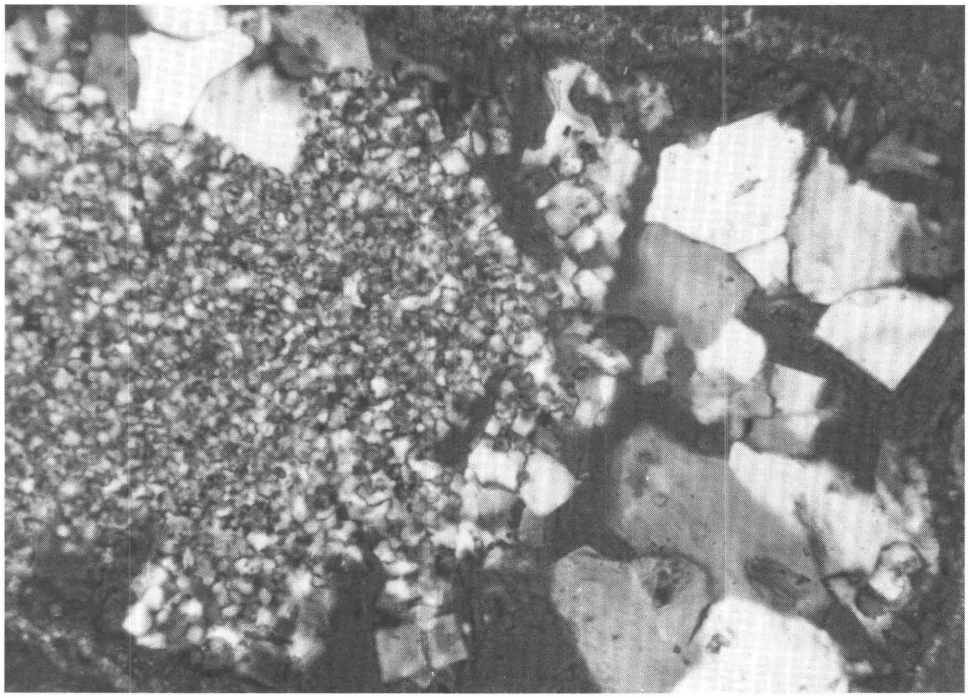

Figure 11. Photomicrograph (polarized light) of fine-grained, anhedral and coarse-grained, euhedral alunite filling void space. Note that the carried borders in the upper left corner suggest that the fine-grained alunite is replacing the coarse-grained alunite. The dimensions shown in the photomicrograph are 0.24 x 0.36 mm.

Table 6. Clay-sized minerals detected by X-ray diffraction[1] in lahar, debris avalanche, and glacial deposits

Sample[2]	Location	Minerals identified by x-ray diffraction[3]
1.	1921 debris avalanche--Crofton Creek	plg/al/sm, kaol/aug
2.	Salt Creek lahar--upper Salt Creek	plg/al, sm/kaol
3.	Salt Creek lahar--Crofton Creek	plg//al, sm
4.	Salt Creek lahar--upper Cascade Creek	plg//sm
5.	Salt Creek lahar--Cascade Creek at Salt Creek	plg//sm, al, kaol?
6.	Veneer, Salt Creek Lahar--Cascade Creek at White Salmon River	plg//sm, aug, ht?
7.	Salt Creek lahar--Cascade Creek at White Salmon River	plg/al/aug
8.	Salt Creek lahar--upper Trout Lake lowland	plg/al/sm, aug
9.	Weathering zone, Salt Creek lahar--Trout Lake lowland	plg/al/sm, aug
10.	Salt Creek lahar--Trout Lake lowland	plg/al/sm, aug
11.	Salt Creek lahar--Trout Lake at Trout Lake Creek	plg/al/sm
12.	Pre W post P lahar--upper Cascades Creek	plg//aug
13.	"Hyperconcentrated" lahar--Cascade Creek at White Salmon River	plg//kaol, aug
14.	Older lahar--Cascade Creek at White Salmon River	plg//kaol, aug, ht?
15.	Trout Lake mudflow--upper Cascade Creek	plg, al//sm, aug
16.	Trout Lake mudflow--Cascade Creek	plg/al/aug
17.	Trout Lake mudflow--upper Trout Lake lowland	plg/al/kaol, aug
18.	Trout Lake mudflow--Trout Lake lowland at Trout Lake Creek	plg/al/kaol, aug
19.	Upper zone, mudflow--Trout Lake lowland at Trout Lake Creek	plg, al//sm, aug
20.	Lower zone,mudflow--Trout Lake lowland at Trout Lake Creek	plg/al/sm, aug, ht?
21.	Trout Lake mudflow--Trout Lake lowland at Trout Lake Creek	plg/al/sm, aug, kaol?
22.	Upper zone, Trout Lake mudflow--lower Trout Lake lowland	plg/al/aug
23.	Lower zone, Trout Lake mudflow--lower Trout Lake lowland	plg/al/sm, aug

[1] Powder diffractometer with Copper Kalpha radiation was used.

[2] Samples in table 6 correspond with those in table 5.

[3] Plg, plagioclase; aug, augite; ht, hematite; al, alunite, sm, smectite; kaol, kaolinite. Slash suggests decrease in abundance; double slash suggests marked decrease in abundance; question mark denotes questionable presence of mineral.

section (units 2 and 3, measured section 1) are not obviously correlative to other lahars in the White Salmon River drainage. A thin veneer of the Salt Creek lahar (unit 4) drapes hillsides and terraces more than 30 m above stream level in this area; this lahar is discussed later in this section. The Trout Lake mudflow is not present in measured section 1.

The deposit of the older lahar (unit 2, measured section 1) differs from other lahars observed in the White Salmon River drainage because it is better sorted and many of its clasts are more rounded. In one sample (No. 14, table 5; unit 2, fig. 12), the sand-size fraction (40 percent by weight) and gravel-sized fraction (50 percent) predominate; the phi standard deviation (Inman, 1952) of the sample is 3.2. Approximately 2 percent of entrained andesite clasts contain secondary minerals. XRD of the clay fraction indicates plagioclase and trace kaolinite.

A crudely stratified lahar (unit 3, measured section 1) is exposed in several road cuts and stream banks in lower Cascade Creek. This deposit forms a terrace about 12 m above the present riverbed near the confluence of Cascade Creek and the White Salmon River that is restricted to valley bottoms. The matrix is composed of sand- and granule-sized particles; scattered throughout the matrix are subrounded pebbles, cobbles, and boulders as large as 80 cm in diameter.

The texture of one sample taken from the matrix of the deposit is shown in figure 12 (unit 3) and table 5 (No. 13). The sand-sized fraction constitutes 50

Table 7. Radiocarbon dates pertaining to lahar deposits near Mount Adams

Sample	Radiocarbon Date (years B.P.)	Description of sample and locality
W-5065	<200	Wood collected from an exposure of the Salt Creek lahar along Cascades Creek about 800 m upstream from its confluence with Salt Creek.
UW-126[1]	5,070–260	Wood from a tree stump near the base of the Trout Lake mudflow in an exposure along the White Salmon River about 2 km downstream from its confluence with Trout Lake Creek.
W-5066	5,300 –100	Wood collected from the Trout Lake mudflow along the bank of Trout Lake Creek, 800 m above its confluence with the White Salmon River.
W-5064	> 38,000	Wood collected near the base of a lahar, 30 m thick, about 500 m up the Underwood Heights road from its intersection with Washington State Highway 14.

[1] Sample (Hopkins, 1976) analyzed at the University of Washington.

percent, the gravel-sized fraction 47 percent (21 percent granule-sized), and the silt- and clay-sized fraction together only 3 percent of the sample by weight. The phi standard deviation is 2.1. This deposit (unit 3, measured section 1) is restricted to valley bottoms. The crude stratification, dominant sand and granule particle size, and low sorting coefficient suggest deposition by a lahar in the beginning stages of transformation to hyperconcentrated flow. In deposits from the 1980 eruptions of Mount St. Helens, Janda and others (1981) and Scott (1985, 1988) noted transitions from lahar to hyperconcentrated flow. Gravel clasts in unit 3 are nearly all (96 percent) massive, unaltered andesite from Mount Adams. Clay-sized minerals in the matrix include plagioclase and a trace of augite (No. 13, table 6). The lack of hydrothermally altered clasts indicates that the flow which produced the deposit did not begin as an avalanche of hydrothermally altered debris. Its source is unknown. The lahar could have formed when hot rock moved over ice and snow during an eruption.

Unit 3 is locally oxidized to a depth of about 50 cm. Where present, this weathering zone is characterized by faint, yellowish discoloration but little

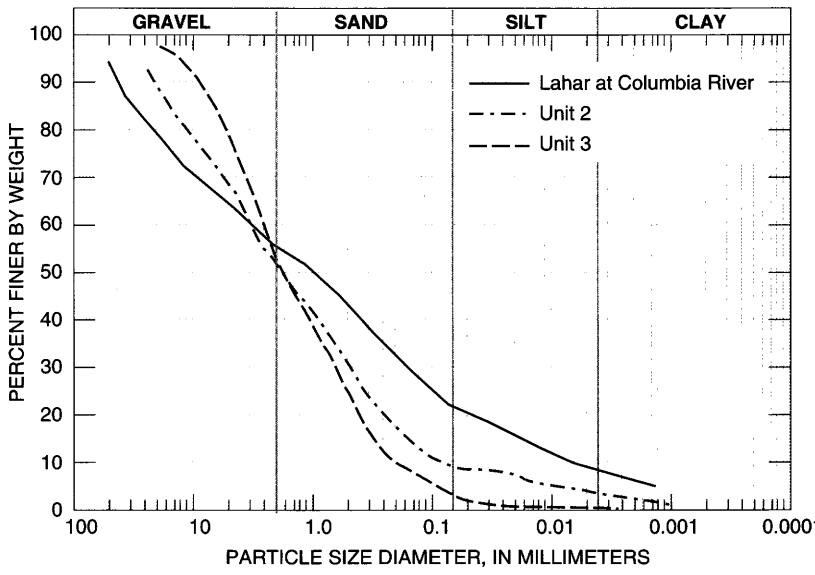

Figure 12. Cumulative curves of the size distribution of grab samples of the lahar near the Columbia River and of two lahars (units 2 and 3, measured section 1) in Cascade Creek about 100 m above its confluence with the White Salmon River.

Measured section 1

[South bank of Cascade Creek near its confluence with the White Salmon River, SW NE SW Sec. 7, T7N, R10E]

Unit		Thickness (centimeters)
4	**Salt Creek lahar:** Pebbles, cobbles, and boulders as large as 50 cm in diameter in a yellowish-brown (10YR 5/4) matrix of sand, silt, and clay that veneers all other deposits in the section	20
3	**Lahar:** Subrounded pebbles, cobbles, and boulders as large as 80 cm in diameter in a pale brown (10YR 6/3) matrix of silt, sand, and gravel, which is faintly stratified; lower contact is sharp	210
2	**Lahar:** Subrounded to subangular cobbles and boulders as large as 30 cm in diameter in a light-brownish-gray to light-yellowish-brown (10 YR 6/2 to 10 YR 6/4) matrix of sand, silt, and clay; lower contact is sharp	530
1	**Diamicton:** Subrounded pebbles, cobbles, and boulders as large as 30 cm in diameter in a grayish- to dark-grayish-brown (2.5Y 5/2-2.5Y 4/2) matrix of sand, silt, and clay and interbedded lenses of sand and silt	410

translocation of clay or weathering of clasts. Comparison of this soil with soils on Evans Creek Drift elsewhere suggests a late glacial to middle Holocene age. Because the lahar deposits are located upstream from moraines of the Evans Creek glaciation, units 2 and 3 are younger than the Evans Creek maximum stand. Thus, the lahars could have occurred during the late Pleistocene retreat of glaciers or later, during ice-free time. Precise age of the lahars is unknown.

Trout Lake Mudflow

The Trout Lake mudflow is the largest postglacial lahar known to originate from Mount Adams. It began as a slope failure high on the southwest flank of Mount Adams where the accumulation zone of the White Salmon and Avalanche Glaciers are now located, flowed down tributaries to the White Salmon River, then followed the river valley southward (fig. 13). The mudflow now occupies about 15 km^2 of the White Salmon River valley near Trout Lake (plate 2). Husum, Washington, nearly 60 km downstream from Mount Adams, marks the maximum known extent of the mudflow.

The distribution, age, and origin of the Trout Lake mudflow have previously been discussed by Jones (1960) and Hopkins (1976). Jones (1960) described the mudflow in a report for a proposed White Salmon River hydroelectric project. His description was based on numerous test holes at proposed dam sites and on the results of several seismic surveys. Hopkins (1976) named the Trout Lake mudflow, mapped its distribution in the Trout Lake area, and dated it. Jones (1960) and Hopkins (1976) both concluded that the deposit was a lahar because of its poor sorting, its lack of stratification, and its distribution as a flat-surfaced lobe in the White Salmon River valley. Hopkins (1976) suggested that the mudflow originated high on the west flank of Mount Adams at the head of the White Salmon River catchment.

The Trout Lake mudflow has been dated at 5,070 ± 260 years B.P. (Hopkins, 1976; sample UW-126, table 7) and 5,300 ± 100 years B.P. (this study; sample W-5066, table 7). Correcting these two dates for variations in atmospheric CO^2 yields intervals of 6,177 to 5,497 and 6,270 to 5,949 years B.P. at the 67 percent (one sigma) confidence level (Pearson and others, 1986). The actual age of the deposit is probably near 6,000 years B.P.

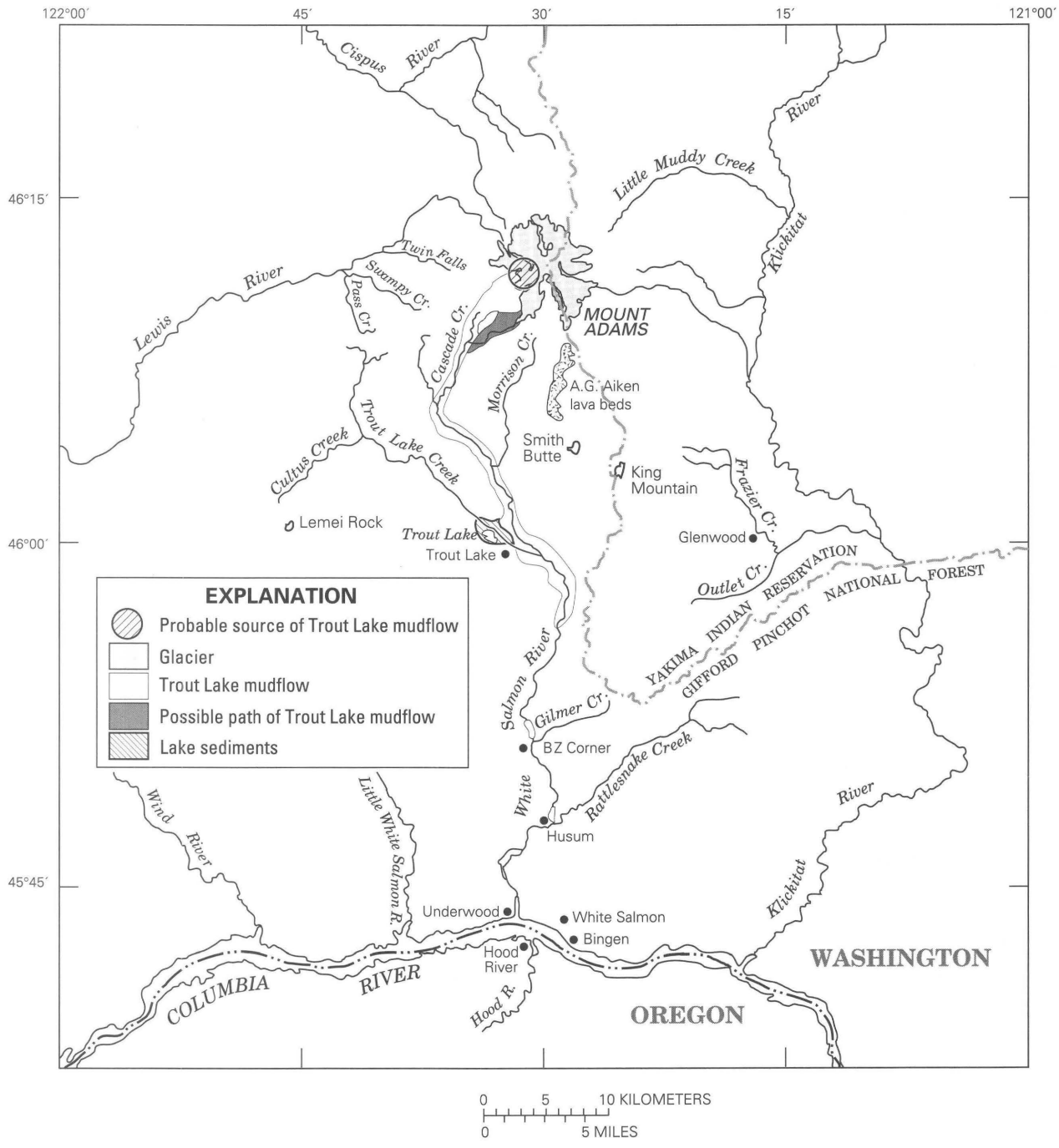

Figure 13. Mount Adams and White Salmon River drainage illustrating the source and path of the Trout Lake mudflow.

Distribution, Characteristics, and Volume

The Trout Lake mudflow was traced upstream as far as neoglacial moraines of the White Salmon and Avalanche Glaciers. In Cascade Creek it underlies or crops out just downstream from the moraines. It also underlies moraines of Avalanche Glacier in Salt Creek drainage. Tephra set Y commonly overlies the deposit upstream from Trout Lake. The deposit is poorly sorted, unstratified, not graded, and contains abundant clasts of hydrothermally altered andesite (fig. 14). Veneer deposits, up to several tens of centimeters thick, crop out at scattered localities on hillsides and high terraces in valleys below timberline. Along Cascade Creek, between Salt Creek and the White Salmon River, younger lahars obscure the Trout Lake mudflow at most localities. No deposits of the Trout Lake mudflow have been found in the upper narrows of the White Salmon River although it flowed through that reach. The most extensive deposit of the Trout Lake mudflow, a lobe nearly 12 km long and a maximum of 2 km wide, underlies the Trout Lake lowland (plate 2). Drilling logs indicate that the deposit is up to 20 m thick where the White Salmon River enters the lowland, whereas down valley it is generally 1 to 4 m thick (plate 2).

The Trout Lake mudflow undoubtedly changed the courses of both the White Salmon River and Trout Lake Creek in the Trout Lake lowland. The White Salmon River returned to its former channel incised in bedrock near the distal margin of the Trout Lake lobe. A seismic survey (Jones, 1960) suggests an ancient White Salmon River channel in the upper Trout Lake lowland located at a base level about 15 m below and 100 m farther west of its present location (cross section , plate 2). In the upper Trout Lake lowland, the White Salmon River and Trout Lake Creek flow along the margin of the lahar

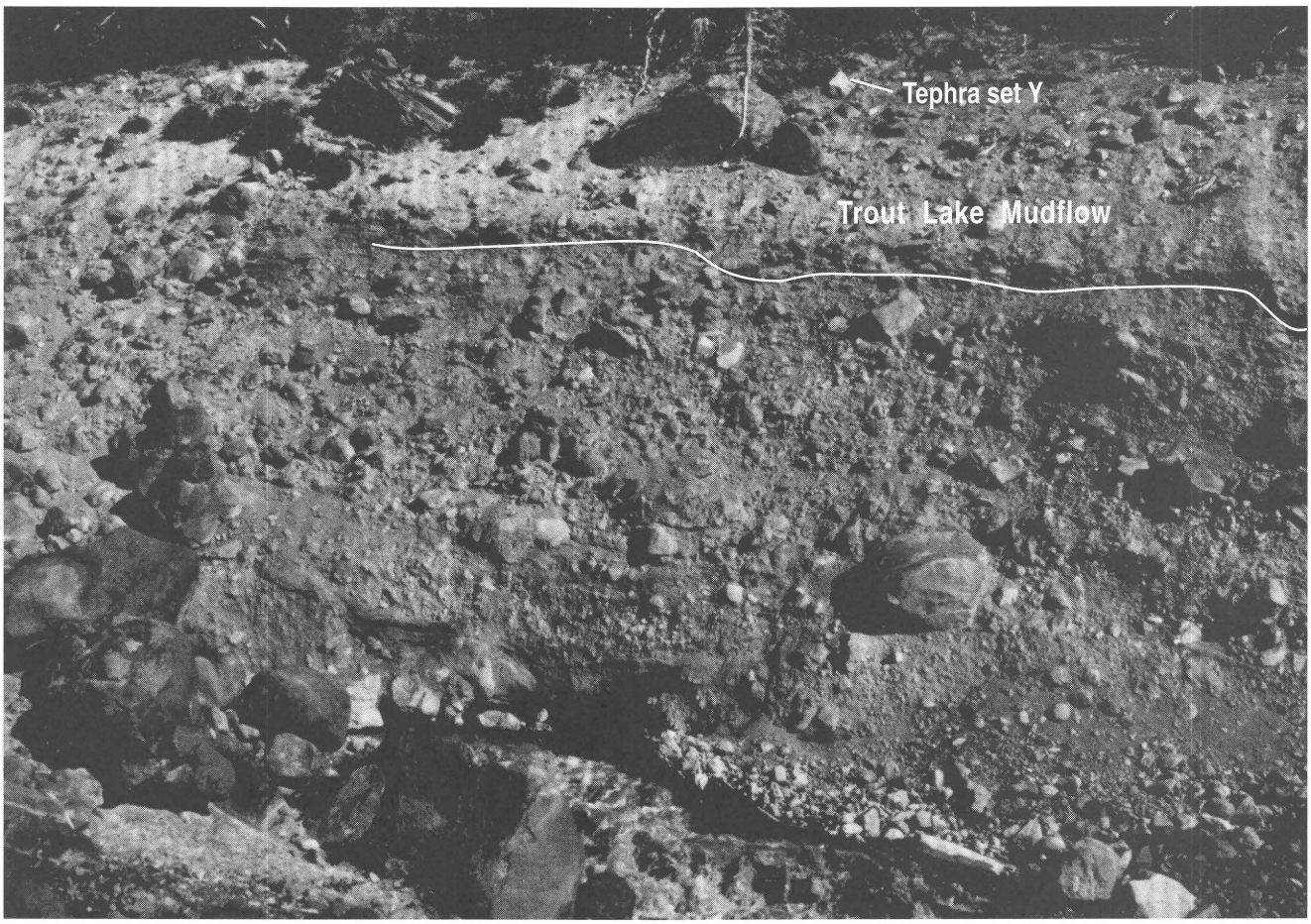

Figure 14. Trout Lake mudflow along upper Cascade Creek near timberline. The deposit is overlain by tephra set Y and underlain by glacial drift. The large boulder in the right-center of the photograph is 1 m across.

Measured section 2

[South bank of Trout Lake Creek near its confluence with the White Salmon River SE SE NW Sec 24, T6N R10E]

Unit		Thickness (centimeters)
7	**Duff and soil:** Silty, fine-grained sand; dark brownish gray (2.5Y 4/2) dry; contains roots and abundant organic matter; lower contact is gradatioal	13
6	**Lahar:** Subrounded, occasionally subangular pebbles and cobbles as much as 15 cm in diameter in a matrix of sandy silt, which is pale brown to yellowish-brown (10YR 6/3-10YR 5/4); lower contact is sharp	40
5	**Duff and soil:** Silty to fine-grained sandy; dark brownish gray (2.5Y 4/2) dry; roots and organic matter are common; lower contact is gradational	25
4	**Trout Lake mudflow:** Subangular to subround pebbles, cobbles, and boulders as large as 2 m in a slightly plastic matrix of sandy silt that is brown to yellowish brown (10YR 5/3-10YR 5/4), brownish-yellow mottles (10YR 5/6) are common particularly in the upper 1.5 m; contains abundant wood fragments. An orange band indurated by iron oxide is situated at the basal contact; this contact is sharp	320
3	**Duff:** Sandy, silty; contains considerable quantities of organic material dark gray, mottled orange	3
2	**Sand:** Fine to medium-grained, probably alluvial. Near the upper contact an orangish-brown layer may represent reworked Mazama ash	10-50
	Erosional unconformity	
1	**Basalt of Ice Cave:** Dark gray, highly vesicular olivine basalt	> 100

where its surface is slightly convex in the upper Trout Lake lowland; near the confluence they have incised into the lahar (plate 2). The White Salmon River has dissected the mudflow and underlying alluvium throughout much of the lowland; locally it is incised into 1 to 2 m of the basalt of Ice Cave.

Emplacement of the mudflow dammed Trout Lake Creek to form Trout Lake. The resulting lacustrine and interbedded alluvial sediments now occupy about 3 km^2 of the Trout Lake lowland (plate 2). The areal extent of the ancient lake is based on the distribution of lacustrine silt, sand, and clay underlying a swampy tract of Trout Lake Creek valley. Much of this tract is now underlain by alluvium, but drilling (Jones, 1960) that penetrated lacustrine silt and clay underlying the alluvium (plate 2) shows the maximum extent of the lake at cross-section *B-B´*. The cross-section indicates that lacustrine silt and clay, overlain by alluvial sand and gravel, filled a once-larger prehistoric Trout Lake.

The deposit has a well-defined eastern margin; the western margin is less well defined. The boundary is indistinct along most of its west and distal margin where the slope of the valley side is gentle. Locally, isolated hills of Ice Cave basalt protrude through the surface of the deposit.

The Trout Lake mudflow is exposed in cross section along Trout Lake Creek and White Salmon River in the Trout Lake lowland. It overlies alluvial sands and gravels, intracanyon Ice Cave basalt, or older basalt. In the northern Trout Lake lowland a younger lahar (measured section 2, plate 2) or lacustrine sediments locally overlie the lahar.

The lack of conspicuous internal stratification in the Trout Lake mudflow suggests that it was deposited as a single unit. In nearly every outcrop in the Trout Lake lowland, in which both the base and top of the deposit are exposed, pebble-, cobble-, and boulder-sized clasts, decrease in number and size from bottom to top (fig. 15). The upper 1 to 2 m of the mudflow includes yellow patches of very high chroma; commonly the lower boundary of this zone is distinctly bounded by one to several layers of iron-oxide-cemented hardpan. The iron-oxide bands probably reflect fluctuations of the water table. Wood fragments, including stems, limbs, entire tree trunks, and in one place, overridden stumps in the original growth position are common below the hardpan. The abundance of incorporated wood fragments indicates that much of the Trout Lake lowland was heavily forested at the time of the mudflow. Although wood fragments are not present above the hardpan, molds of wood fragments are numerous, the wood having apparently dissolved. The cause underlying this difference in wood preservation is presently unclear; possibly, bacterial action above the water table led to wood breakdown. Numerous small voids in the matrix of the lahar are air bubbles entrapped during flowage.

Deposits of the mudflow are located within the lower gorge of the White Salmon River near BZ Corners and Husum; reconnaissance mapping revealed no deposits of the Trout Lake mudflow further down valley than

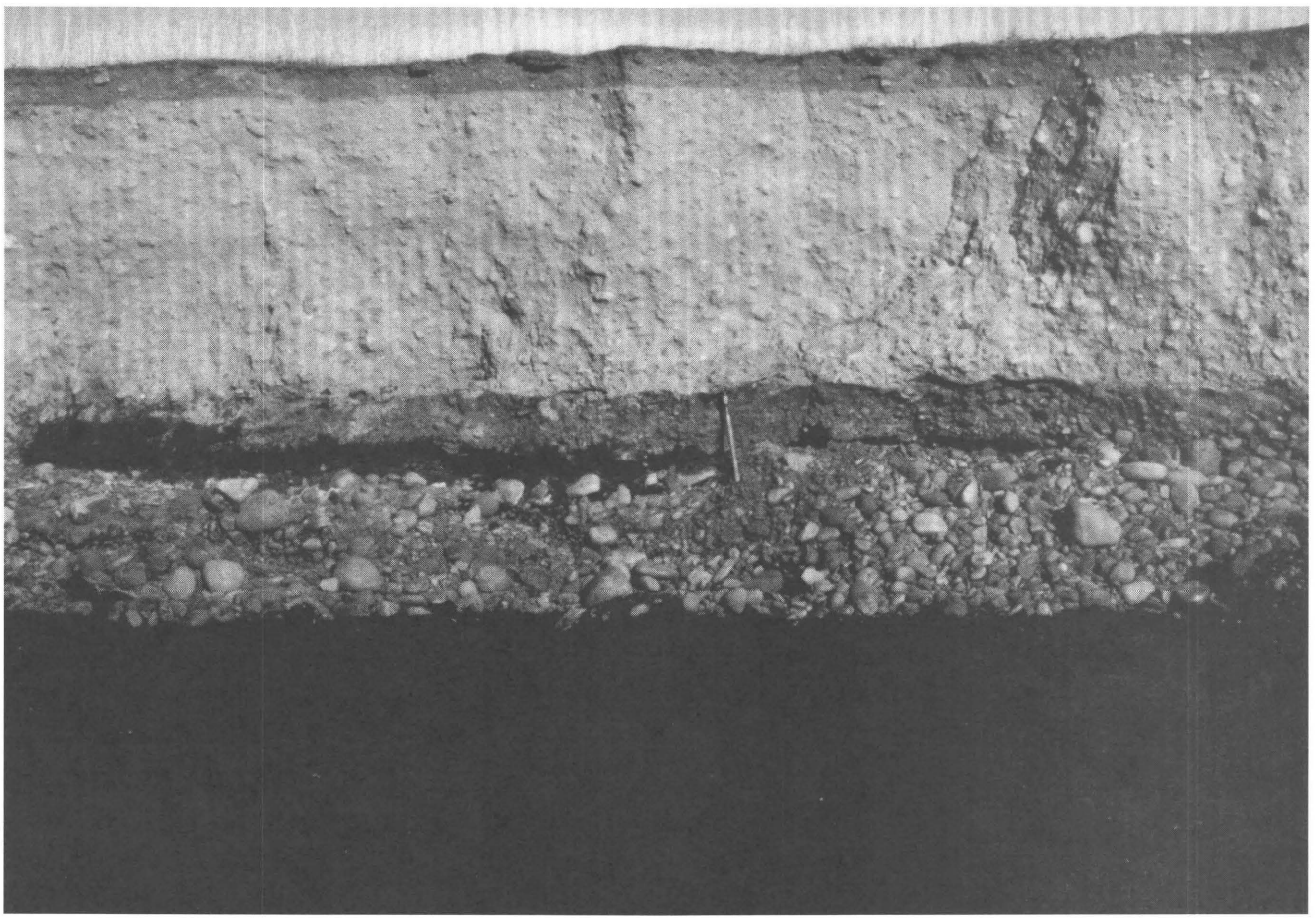

Figure 15. Exposure in the Trout Lake lowland of the Trout Lake mudflow resting on fluvial gravel. Note the normally graded top. The dark zone at the top of the mudflow is soil. Shovel for scale.

Husum. At Husum, the deposit, which is as thick as 3 m and overlies more than 1 m of alluvium, forms levees 3 to 5 m above present river level. Here the deposit is poorly sorted and not obviously stratified. Of the gravel clasts, only pebbles are commonly matrix supported. The presence of clast-supported cobbles and boulders suggests that some winnowing of the matrix material has occurred, possibly in response to increased water during transport. Cobble- and boulder-sized clasts exhibit more rounding than those observed in the Trout Lake lowland.

The lahar underlies about 15 km^2 in the Trout Lake lowland, where it has an average thickness of about 4 m. The mudflow originally underlaid approximately 12 km^2 of the Salt Creek and Cascade Creek valleys in a layer that varied from veneers 10 to 20 cm thick to valley fills several meters thick (averaging about 0.5 m in thickness). The estimated total volume is about 66 million cubic meters.

Texture, Composition, and Mineralogy

Nine samples of the Trout Lake mudflow collected at seven sites along streambanks were analyzed for grain size distribution (samples 15-23, table 5). At two of these sites in upper Cascade Creek, the lahar occurs as a thin veneer or is only preserved in pockets; at the five sites in the Trout Lake lowland where the mudflow is more than 3 m thick, samples were collected from depths greater than 2 m. At two sites, samples (Nos. 19 and 22) were collected from the upper 1 m of the lahar. No clasts larger than 20 cm were collected although such clasts are common in the deposit. Median phi diameter, phi standard deviation, and the texture of the samples are shown in table 5; the clay-sized fraction of the samples ranges from 3 to 8 percent, the silt-sized fraction from 5 to 12 percent, the sand-sized fraction from 25 to 44 percent, and the gravel-sized fraction from 38 to 62 percent. Phi standard deviations range from 3.9 to 5.8 and average 4.5. No change of texture with increasing distance from the source is apparent (fig. 16). Because of its high clay content the Trout Lake mudflow behaved as a cohesive lahar.

Samples taken from both the upper and lower zones of the lahar, at two sites in the Trout Lake lowland where the deposit is 3 to 4 m thick, exhibit no apparent trend in phi deviation or in percent sand, silt, and clay (samples 19 and 20, samples 22 and 23, table 5). This result seems to contradict observations that suggest normally graded tops. However, the samples from a site 35 km downstream indicate a coarser gravel fraction at the base than at the top of the lahar (fig. 16). At another site 30 km downstream, no apparent trend in texture is apparent from top to bottom. The contradiction between textural measurements and observations at the site 30 km downstream results from textural sampling techniques which insufficiently represent clasts 20 cm and larger. The observations at these two sites suggest that normal grading, common in this lahar, is due to the downward decrease in gravel-sized particles.

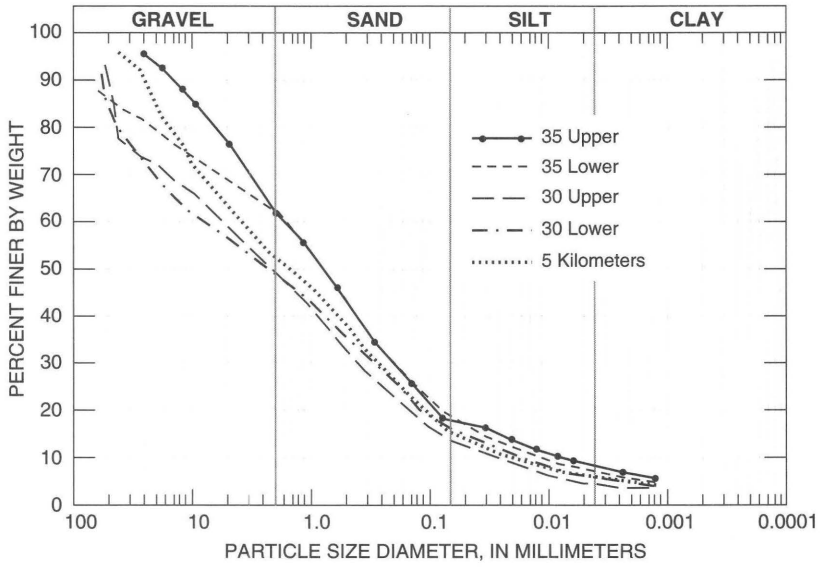

Figure 16. Cumulative curves of the size distribution of samples of the Trout Lake mudflow. Numbers indicate distance in kilometers from source. Denotation of upper or lower indicate grab samples that were taken from the upper or basal meter of the deposit.

Table 8. Lithology of pebble-sized clasts from lahars and debris avalanche of Mount Adams

Deposit	Andesite from Mount Adams				Total	Olivine basalt	Other
	Fresh	Affected by hydrothermal alteration	Strongly affected by hydrothermal alteration	Reddened by oxidation of iron minerals			
Lower part of Trout Lake mudflow in the Trout Lake lowland	56/70[1]	14/18[1]	4/5[1]	6/7[1]	80	16	4
Upper part of Trout Lake mudflow in the Trout Lake lowland	33/40[1]	27/33[1]	22/27[1]	0/0[1]	82	17	2
Salt Creek lahar in Cascade Creek	62/67[1]	16/17[1]	5/5[1]	10/11[1]	93	7	0
Salt Creek lahar in Trout Lake lowland	48/59[1]	22/27[1]	6/7[1]	6/7[1]	82	14	4
Lahar in Cascade Creek (500 - 2,500 yrs. B.P.)	77	15	1	7	100	0	0
1921 debris avalanche in Salt Creek in Salt Creek	38	46	12	4	100	0	0

[1] Number above slash is the percent of total clasts; number below slash is percent normalized to total andesite.

The most common lithologies in the Trout Lake mudflow are hypersthene augite andesite from lava flows and breccias of Mount Adams, and olivine basalt from lava flows of small, adjacent volcanic centers (table 8). No basalt clasts were noted in deposits of the mudflow within 10 km of the source. The presence of basalt clasts within the lahar in the Trout Lake lowland suggests that as the lahar moved away from the volcano, it incorporated alluvium, colluvium, and fragments of bedrock, some of which originated from sources other than Mount Adams. In following down valley, the lahar could have incorporated alluvium that also contained andesite so that the presence of about 20 percent basalt in lahar deposits indicates a minimum amount of material incorporated.

Andesites from Mount Adams include some rocks that are gray and massive, some that are very dark gray and vesicular, and others that are dark reddish gray owing to oxidation of iron minerals. Andesite clasts may be partially to totally altered by hydrothermal processes. Proportions of the rock types and the degrees of alteration of the volcanic clasts of Mount Adams measured at two sites in the Trout Lake lowland are given in table 8. Andesite that has been strongly affected by hydrothermal alteration tends to be less dense than fresh andesite; probably as a result, this altered rock makes up a greater proportion of the clasts in the upper part of the mudflow (table 8).

XRD patterns of clay-sized minerals from the matrix of the lahar reveal the presence of plagioclase and pyroxene as primary minerals and secondary minerals such as smectite, kaolinite, and alunite (Nos. 15-23, table 6).

Source and Origin

Presently, the cirque of Avalanche and White Salmon Glaciers (fig. 17) is the only possible source in the White

Presently, the cirque of Avalanche and White Salmon Glaciers (fig. 17) is the only possible source in the White Salmon River drainage for hydrothermally altered clasts and distinctive secondary minerals such as alunite, kaolinite, and smectite. Thus, slope failure from the area of the cirque is the only way in which a lahar with this composition could have been formed.

There is no independent evidence to suggest that the Trout Lake mudflow was triggered by an earthquake, a phreatic eruption, or a magmatic eruption. Nonetheless, seismic and explosive phreatic activity that

accompanies most eruptions would increase the probability of a slope failure such as that which initiated the Trout Lake mudflow. Physical stratigraphy indicates that several flank lava flows occurred during the several-thousand-year interval that includes the time when the Trout Lake mudflow occurred. Dates however, are too imprecise to prove that the flows occurred at the same time. Progressive hydrothermal alteration near the summit of Mount Adams would have weakened source rocks before initiation of the Trout Lake mudflow. Stability could have been further diminished through changes in pore-pressure gradient of subsurface groundwater. Stability of the altered rock mass could also have been lessened by glacial undercutting or by increases in stress owing to a snow and ice overburden.

Post-P, pre-W Lahar

A lahar, which overlies tephra set P and underlies tephra layer W, is exposed along stream banks in upper Cascade Creek at altitudes between 1,280 and 1,900 m (plate 2). The deposit is lobate in form, several hundred meters wide, and 4 km long with an irregular surface. Its margins are abrupt and steep sided; streams now flow along these margins. The deposit presently overlies 1.4 km^2 of the Cascade Creek valley. Assuming an average thickness of 3 m, its volume is estimated to be about 4.2 million cubic meters.

The deposit is an unsorted mass of subrounded to subangular pebbles, cobbles, and boulders up to 1 m across in a brownish-gray, silty-sand matrix. Poor

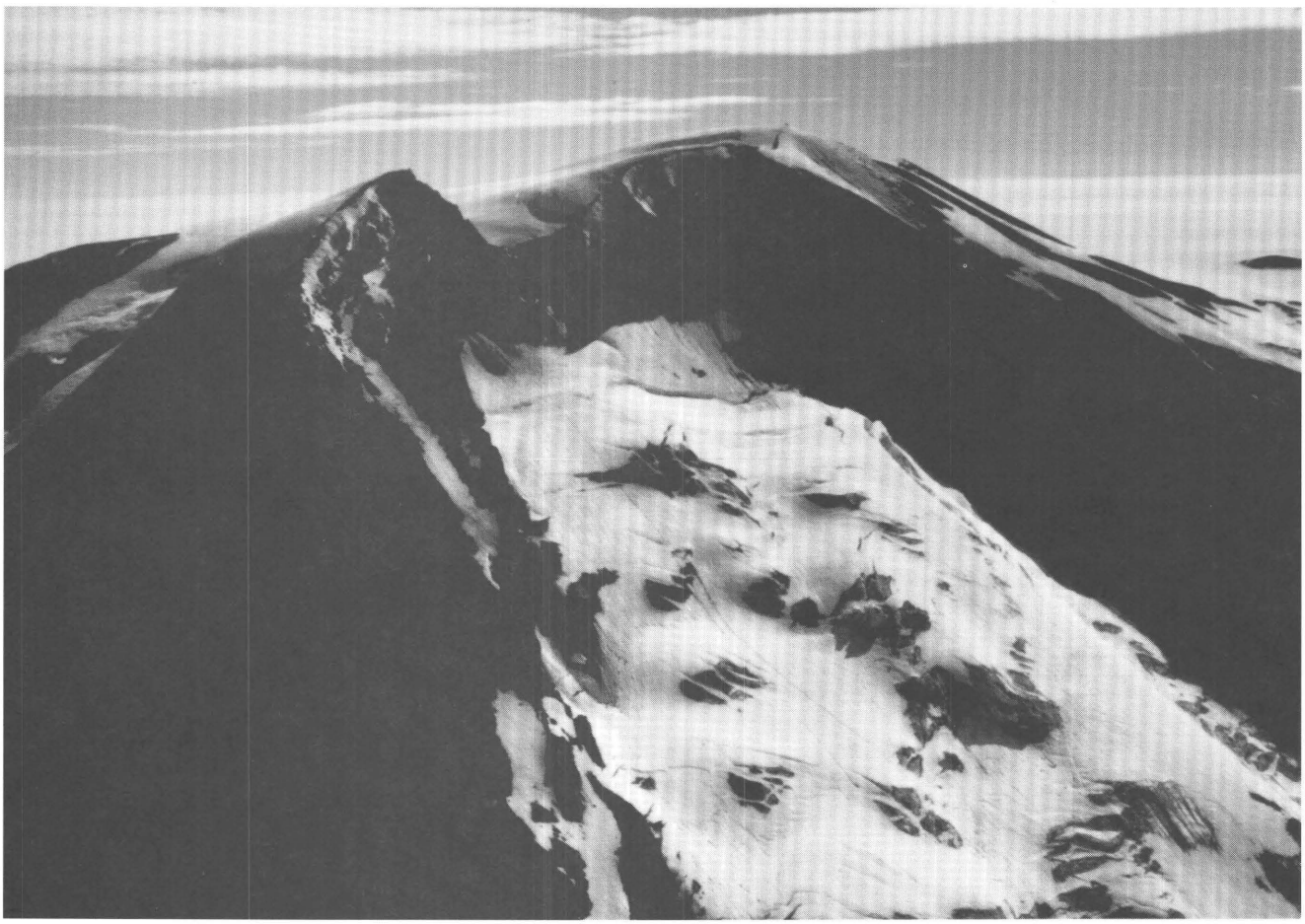

Figure 17. View eastward toward the cirque that forms the accumulation zone of the White Salmon and Avalanche Glaciers. The Pinnacle is left of center and the summit of Mount Adams is slightly right of center. This cirque is the source area of the Trout Lake mudflow. The west-facing cliffs below the summit are the source of the Salt Creek lahar and the debris avalanche of 1921.

sorting and lack of interbedded gravels and sands indicate that it is a single depositional unit. The clasts, all of which are andesite from Mount Adams, are commonly massive and rarely scoriaceous. The proportion of clasts that have been hydrothermally altered is smaller than for either the Trout Lake mudflow or the Salt Creek lahar (table 8). An XRD pattern of the clay-sized fraction shows fresh plagioclase and a trace of augite (No. 12, table 6). The textural characteristics of the deposit are shown in figure 18 and table 5 (No. 12). Sand-sized (35 percent) and gravel-sized (57 percent) fractions are predominant; the silt-sized (5 percent) and clay-sized (2 percent) fractions are minor; the phi standard deviation of the sample is 3.6 (No. 12, table 5).

A lack of hydrothermally altered clasts, breccia blocks, and secondary minerals in the clay-sized fraction suggests that this lahar did not result from avalanches of hydrothermally altered rock on the slopes of Mount Adams. The proportion of altered versus fresh andesite in this lahar resembles that of neoglacial till. However, the morphology, distribution, and age of the deposit indicate that it cannot be till. It could have been derived from till, but its place and manner of origin are unknown.

Salt Creek Lahar

A lahar overlying tephra layer We is exposed along stream banks of Salt Creek below an elevation of 1,700 m. This deposit is herein informally named the Salt Creek lahar for its type locality. The lahar is distributed almost continuously along valley bottoms between an elevation of 1,700 m in Salt Creek and 900 m at the head of upper White Salmon River narrows. The lahar extends into the Trout Lake lowland, more than 30 km from its source (plate 2).

At scattered localities, the Salt Creek lahar overlies 2 to 3 cm of tephra layer We, erupted in AD 1482 (Yamaguchi, 1983). Soil developed on the lahar surface consists of duff and A horizon, directly resting on unoxidized C horizon. Wood contained within the lahar yields a radiocarbon age of less than 200 years (W-5065, table 7). The radiocarbon correction curve of Stuiver and Becker (1986) indicates that the wood has a calendar age of about AD 1660 or younger. Tree stumps on the surface of the lahar exhibit up to 195 tree rings. At one locality on the lahar surface which was logged in 1957, tree stumps were observed having 175 and 177 growth rings. If the trees reestablished quickly, the lahar probably occurred in the later half of the 18th century.

Distribution, Character, and Volume

The lahar along Salt Creek, characteristically 1 to 2 m thick, lacks sorting and internal stratification. The deposit comprises an unsorted mass of pebbles, cobbles, and boulders as large as 1.5 m enclosed in a non-plastic matrix of sand, silt, and clay. It shows no gradation in size or number of gravel-sized clasts from bottom to

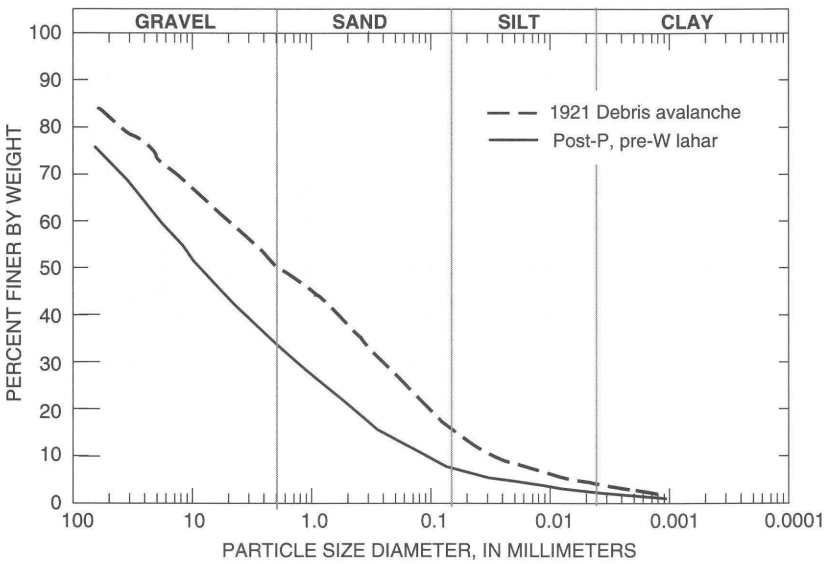

Figure 18. Cumulative curves of the size distribution of spot samples of the lahar that occurred between 500 and 2,500 years B.P. and of the debris avalanvche that occurred in 1921 A.D.

top. Clasts are typically subangular. The lahar matrix is brown to dark yellowish brown (10YR 5/3 to 10YR 4/4), although a more intense chroma (10YR 5/6) is conspicuous in outcrop. The lahar generally lacks wood fragments; however, in one Cascade Creek outcrop 300 m upstream from its intersection with Salt Creek, numerous stems, branches, and logs as large as 2 m in diameter are common.

The Salt Creek lahar left veneers of coarse material near timberline on Crofton Ridge and on the ridge that divides Cascade Creek and Salt Creek (fig. 1). Veneer deposits on valley sides in topographically high areas and in some valley bottoms are easily recognized by the presence of a large proportion of hydrothermally altered clasts. Although these deposits must initially have contained a fine-grained matrix, some of them now lack it. On the steeper slopes some of the muddy matrix probably drained downslope. At Mount St. Helens in 1980, lahars formed bouldery lag deposits draped by thin coats of muddy sand (Janda and others, 1981). Similar thin, fragile coats on deposits of the Salt Creek lahar could have been present but have since eroded away. Mounds 1 to 2 m high and as much as 5 m across, many of which are streamlined in the direction of flow, dot low terraces. Most of the mounds contain cores of breccia and fragmental andesite.

The highest summit of Croften ridge (fig. 1) is about 30 m higher than the saddle that connects it to the southwest flank of Mount Adams. Hydrothermally altered clasts on this small summit and along the narrow ridge were left behind as lag deposits when the lahar, moving at an oblique angle with respect to the ridge, overtopped it. The equation,

$$v^2 = 2gh \ (v = \text{velocity};$$
$$g = \text{gravitational constant}; \ h = \text{height}),$$

suggests a run-up velocity of about 25 m/s. Because of the oblique angle of incidence and the assumption of frictionless flow, the calculated velocity is probably less than the actual velocity.

A lobe of the Salt Creek lahar, approximately 3 km long by 0.5 km wide underlies 1.75 km^2 of the Morrison Creek valley; this lobe is about 8 km from its inferred source (plate 2*A*). The distal margins of the deposit, which exhibit as much as 2 m of relief, commonly are sharply defined and steep-sided; upstream, however, the margins are less distinct, and the deposit is locally preserved. Large boulders of andesite, generally disaggregated, and blocks of breccia dot the flat to irregular surface. Most of these blocks are hydrothermally altered or reddened by oxidation. Another lobe of the lahar is 200 to 300 m wide and extends 3 km or more down a stream channel in upper Cascade Creek valley (plate 2*A*).

Although the morphology of the Salt Creek lahar deposit parallels that of the underlying surface and its margins are indistinct, the lahar surface is readily differentiated from adjacent surfaces by the lack of tephra sets Y and W on it, by the presence of scattered breccia blocks, and by its orange color on aerial photographs.

Deposits near the confluence of Salt and Cascade Creeks suggest that as the lahar emerged from Salt Creek, it filled the valley to a depth of about 20 m, crossed Cascade Creek, and ran up the opposite valley slope an additional 20 m. This amount of run up suggests a velocity in excess of 20 m/s.

Where the White Salmon River enters the upper narrows, the steep-sided, narrow canyon constricted the flow of the lahar causing it to spill over a low divide, about 50 m above the present river level, into the headwaters of Green Canyon. In the narrows of the White Salmon River, the presence of hydrothermally altered clasts of Mount Adams andesite in tributary valleys and on terraces as high as 55 m above the present river level marks the passage of the lahar.

The Salt Creek lahar crops out along stream banks of the White Salmon River in the upper Trout Lake lowland where it overlies the Trout Lake mudflow (plate 2; fig. 19). This lobe has a width of 1 km, a length of 4 km, and a maximum observed thickness of 4 m. Like deposits upstream, those in the Trout Lake lowland are very poorly sorted and unstratified; unlike upstream deposits, some exposures exhibit faint, normal grading. In the Trout Lake lowland, the lahar exhibits downstream changes in texture. Clasts in overbank deposits exhibit increased rounding and decreased maximum size. Increased rounding probably results from the incorporation of alluvium, whereas decreased size of largest clasts suggests decreased carrying power and an increased ratio of water to debris in the lahar.

Texture, Composition, and Mineralogy

The study of texture of the Salt Creek lahar is based on spot samples collected at ten sites (Nos. 2-11,

table 5). At nine of the sites the deposit was at least 1 m thick; at the other it was about 20 cm thick. The texture of the sample taken from a lahar veneer (No. 6, table 5; fig. 20) indicates depletion of silt- and clay-sized particles and much better sorting compared to those of samples taken from thicker fill deposits. Downstream change in texture (table 9 and fig. 20 includes a decrease in sand, silt, and clay and a corresponding increase in gravel. In addition, mean grain size increases and sorting improves slightly with distance downstream.

The most common lithologies contained in the lahar are andesite from Mount Adams and olivine basalt from nearby volcanic centers (table 8). The percentage of lithologies other than the Mount Adams andesite increases with distance from source (table 9). This indicates that the lahar incorporated alluvium, colluvium, and bedrock from sources other than Mount Adams. Alluvium in the White Salmon River valley consists primarily of pebbles and cobbles. Colluvium consists of similarly coarse particles. Clastic material incorporated by the lahar is likely to consist primarily of coarse clasts. In addition, clasts derived directly from bedrock are likely to be coarse. Erosion and incorporation by the lahar of coarse particles could account for the observed downstream coarsening of texture. In particular, incorporation of alluvial particles could account for increased roundness of clasts seen in the Trout Lake lowland.

The lahar contains many hydrothermally altered massive, scoriaceous, and brecciated clasts of Mount Adams andesite. The proportions of altered andesite are given in table 8.

Of ten clay-sized samples analyzed by XRD for clay mineralogy, only the one taken from nearest the source--above timberline in Salt Creek valley--shows significant proportions of secondary minerals such as smectite, alunite, and minor kaolinite (Nos. 2-11, table 6; fig. 21) . Samples taken downstream contain minor

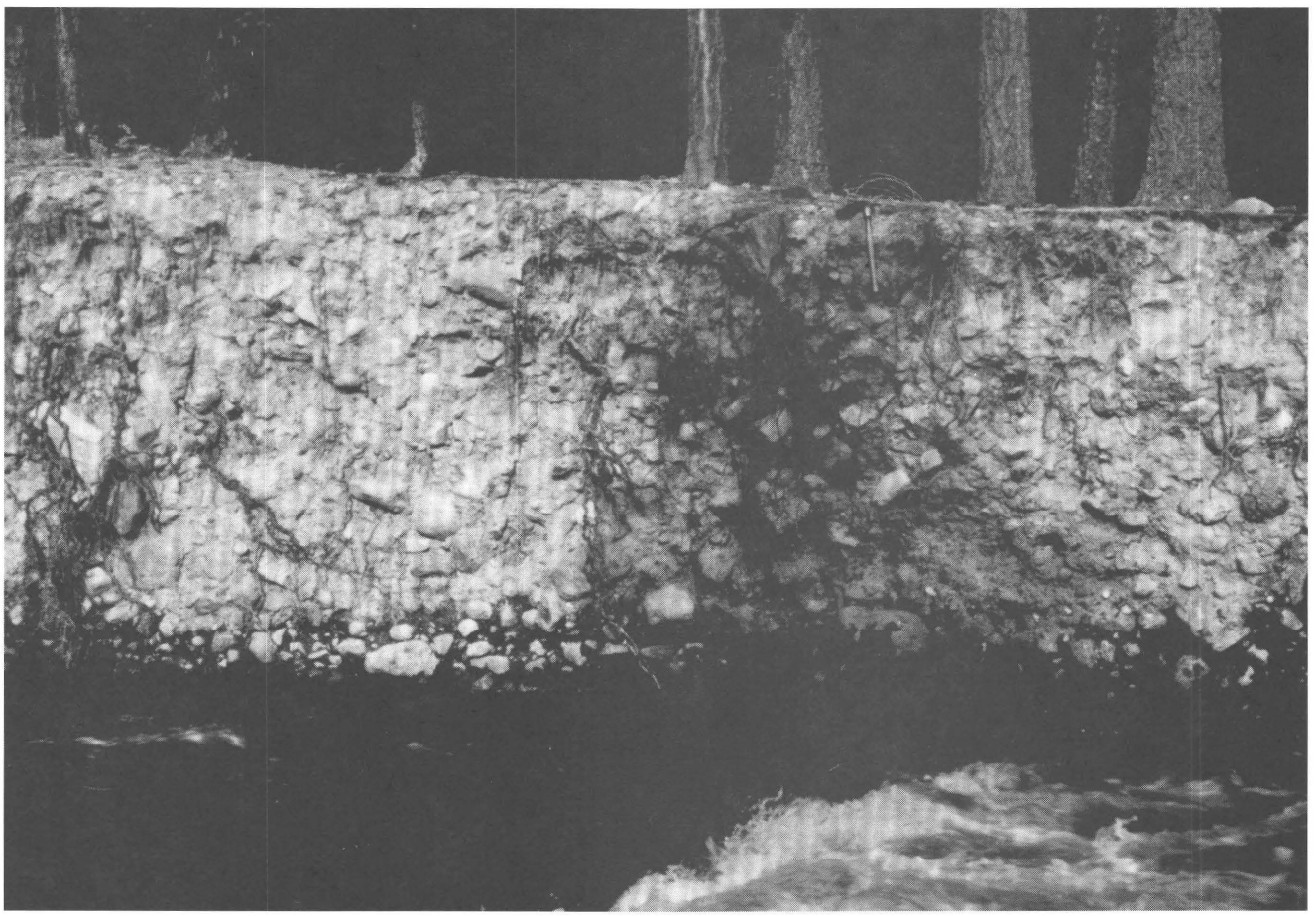

Figure 19. Salt Creek lahar in the Trout Lake lowland (base not exposed). Shovel for scale.

Table 9. Changes in composition and texture of Salt Creek lahar (~200 yrs. B.P) with distance from source. Samples were taken from deposits one or more meters thick except as noted.
[Leaders (—) indicate no data]

Valley morphology	Distance from source	Percent lithology not of Mt. Adams origin	Texture					
			gravel	sand	silt	clay	md_Φ	σ_Φ
Volcano slopes (0 to 50 km)	5	0	51	25	10	4	-1.1	5.0
Glaciated valleys (5 to 16 km)	10	0	42	39	14	5	0.15	4.9
	15	7	46	40	10	4	-1.1	4.3
	15[1]	7	42	51	5	2	-0.14	2.6
Incised bedrock gorge (16 to 27 km)	—	—	—	—	—	—	—	—
Broad lowland valley (27 to 40 km)	28	18	50	38	8	4	-1.1	4.5
	30	---	68	23	6	2	-4.3	4.1
	31	---	73	19	6	2	-4.3	3.9

[1] Sample taken from a veneer deposit about 25 cm thick.

smectite and alunite, and primary minerals such as plagioclase and pyroxene.

The Salt Creek lahar evidently resulted from slope failure of hydrothermally altered rocks in cliffs above Avalanche Glacier. The presence of the lahar near neoglacial moraines indicates that it came from above the moraines; deposition on Crofton ridge and in the valley southeast of the ridge indicates that some debris overtopped the ridge and entered Morrison Creek valley. The lahar in Cascade Creek valley (plate 2) is restricted to one small drainage that heads at Avalanche Glacier. Judging from this distribution, the source of the lahar must have been above Avalanche Glacier. The abundance of hydrothermally altered andesite and the

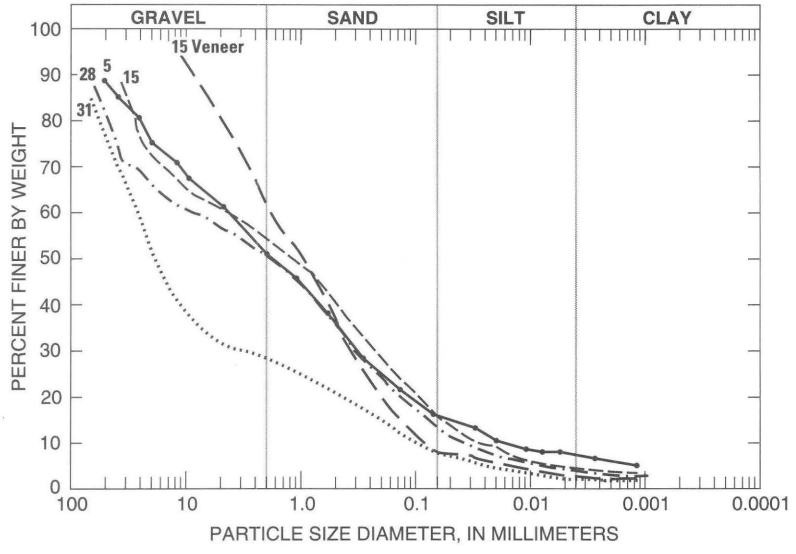

Figure 20. Cumulative curves of the size distribution of samples of the Salt Creek lahar. Numbers indicate kilometers from source. Spot samples were taken from deposits 2 or more meters thick except the one that is denoted veneer, which was taken from a deposit 20 cm thick.

presence of distinctive secondary minerals within the Salt Creek lahar indicates that it began as a landslide of hydrothermally altered andesite. Rocks in cliffs that head Avalanche Glacier (fig. 17) have been severely solfatarized, forming secondary minerals like those detected in the lahar. A cliff in approximately the same place as the west-facing cliff that now heads Avalanche Glacier (fig. 17) was the source of the Salt Creek lahar. This cliff exposes the most strongly altered rock visible on Mount Adams. A slab, approximately 100 m high, 200 m thick and 0.75 km long, collapsing from this cliff today, would equal the volume of debris in the Salt Creek lahar.

1921 Debris Avalanche

Two diamictons crop out along stream banks in upper Salt Creek (fig. 22). Contacts between the two are subtle. Two populations of trees having different ages differentiate the diamictons on adjoining surfaces below timberline. The older diamicton is the Salt Creek lahar and the younger is a debris avalanche that occurred in May, 1921 (Byam, 1921).

The debris avalanche left deposits throughout the upper Salt Creek valley above 1,600 m; it also produced several small lobes which moved down a tributary of Morrison Creek and one lobe that moved more than 2 km down a tributary of Cascade Creek (plate 2). The

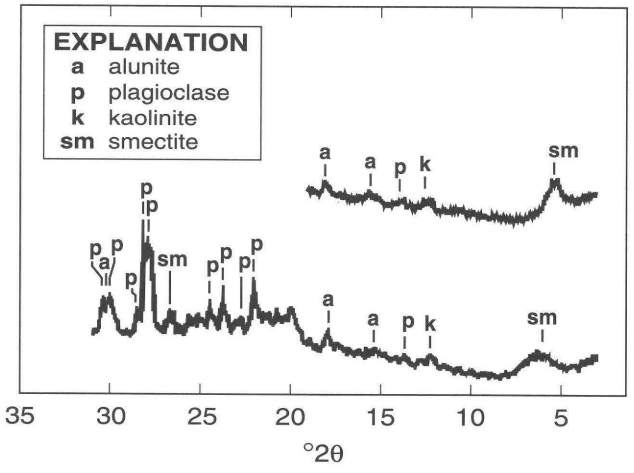

Figure 21.--X-ray diffraction pattern of the clay-sized fraction of a sample No. 2 in tables 8 and 9) of the Salt Creek lahar from upper Salt Creek, showing plagioclase, smectite, kaolinite, and alunite.

avalanche deposits cover about 4 km^2 of the southwestern flank of Mount Adams. An estimated volume of 4 million m^3 is based on an average thickness of 1 m.

The surface of the avalanche deposit is irregular and hummocky. Hummocks are commonly higher in the basin, and one particularly hummocky part of the deposit overlies stagnant ice behind moraines of the Avalanche Glacier. Masses of disintegrating andesite and blocks of breccia as large as 3 x 4 x 6 m are strewn about the surface of the deposit. Areas near the margin of the deposit are covered by scattered pebbles, cobbles, and boulders.

The debris avalanche, as thick as 4 m, contains unsorted pebbles, cobbles, and boulders (as large as 2 m) enclosed in a slightly plastic, yellowish-brown matrix of sand, silt, and clay. The deposit drapes neoglacial moraines and overlies older lahars or outwash beyond the margins of these moraines. Deposits of the 1921 debris avalanche and the Salt Creek lahar are difficult to differentiate above timberline in Salt Creek because of lithologic similarity and the short time elapsed between their emplacement. Below timberline the contacts are readily discernible. All clasts in the avalanche deposit are andesite from Mount Adams. The clasts are brecciated, scoriaceous, or massive; many are hydrothermally altered; and some are brilliantly colored purple, yellow, and white. The proportions of altered clasts are given in table 8. The grain-size distribution of one debris-avalanche sample is given in table 5 (No. 1) and figure 18. The clay-sized fraction is 5 to 7 percent, the silt-sized fraction 8 percent, the sand-sized fraction 36 percent, the gravel-sized fraction 49 percent, and the phi standard deviation 4.4.

The 1921 debris avalanche originated from the west-facing cliff at the head of Avalanche Glacier. The mass moved down the Avalanche Glacier along a narrow path that gradually widened then overrode glacial moraines (fig. 23). Most of the debris moved down Salt Creek while smaller masses descended tributaries of Cascade and Morrison Creeks.

A hydrothermally weakened and already oversteepened cliff face set the stage for slope failure. High pore-water content, as a result of an exceptionally wet winter and spring that preceded the avalanche (Byam, 1921), may have triggered failure. Another possible trigger could have been a small steam explosion. In 1924 an observer reported seeing steam

vents west of the summit, south of the Pinnacle, and above the White Salmon Glacier--an area close to the avalanche source (Phillips, 1941). No steam vents are now present in that area.

Historic Lahars

A small lahar occurred in September 1981, during hot, dry weather and destroyed nearly 100 m of the Round-the-Mountain Trail. The lahar originated near a moraine of Avalanche Glacier and cut a path 10 to 100 m wide nearly 4 km downstream (fig. 24). It formed prominent levees, moved boulders as large as 3 x 3 x 4 m, and destroyed or damaged trees. Some trees were abraded up to 1 m above the deposit surface on their stoss sides and had pebble- and cobble- sized clasts embedded in them; others were bent and completely stripped of bark. A cobble count showed that all of the clasts are andesite. Seventy-eight percent are fresh, 8 percent are reddened by oxidation of iron minerals, and 14 percent are altered hydrothermally--all proportions that are similar to material in the Avalanche Glacier moraine. A glacier outburst flood probably triggered the flow.

This type of lahar is common at Mount Adams. Another lahar having a similar origin occurred on the north side of Mount Adams in Adams Creek during the same hot, dry period. A sequence of four unforested and three forested levees and terraces, deposited by small lahars, are present at the junction of Cascade and Salt Creeks about 8 km downstream from Avalanche Glacier. These lahars clearly postdate the Salt Creek lahar, which occurred in the middle of the eighteenth century. Lack of reforestation on four of the deposits, and the youth of the forest growing on the three others, suggests the lahars probably postdate the 1921 debris avalanche.

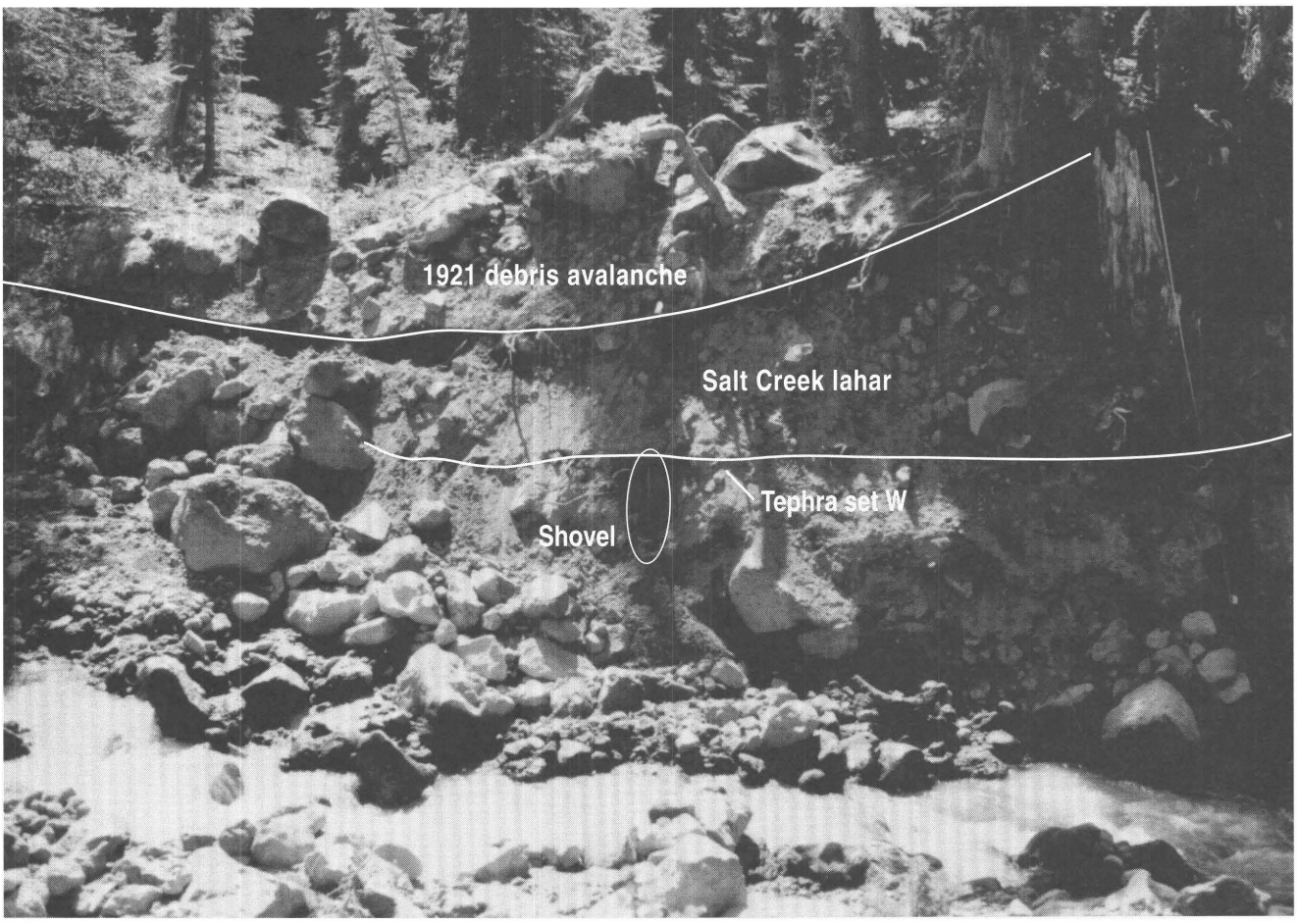

Figure 22. Deposits of the 1921 debris avalanche and the Salt Creek lahar, overlying tephra layer We in upper Cascade Creek. Note the tree (in a diamicton of unknown origin) buried by the Salt Creek lahar. Shovel for scale.

Origin of Cirque on the Southwest Side of Mount Adams

The cirque that is now the accumulation zone for the White Salmon and Avalanche Glaciers (fig. 17) evidently resulted from the slope failure that initiated the Trout Lake mudflow rather than from glacial erosion. The cirque was later enlarged by slope failures that caused the Salt Creek lahar and the 1921 debris avalanche. The Trout Lake mudflow and the Salt Creek lahar can be traced up valley to moraines of the White Salmon and Avalanche Glaciers, which indicates a source area for the lahars above the moraines. The debris avalanche of 1921 was observed to come from the west-facing cliff below the summit crater (Byam, 1921). Further, cliffs of the cirque headwall are the only source within the White Salmon River drainage basin of hydrothermally altered andesite and secondary minerals common in deposits of the flows.

An estimated volume of the cirque is 64 million m^3. The cirque has an approximate area of 0.64 km^2; and its headwall is as high as 180 m. Assuming an average ice thickness of 20 m, the volume defined by the cirque has a vertical dimension that ranges from 20 to 180 m, and averages 100 m; thus, the estimated volume of the cirque is 64 million m^3. The inferred volume of the Trout Lake mudflow is 66 million m^3, that of the Salt Creek lahar is 15 million m^3, and that of

Figure 23. The debris avalanche of May 1921 on the southwest side of Mount Adams. Telephoto taken from Trout Lake on July 4, 1921 (Rusk, 1978, p. 106; *Tales of a Western Mountaineer*). Copyright 1978 by The Mountaineers, 306 2nd Avenue West, Seattle, Washington.

the 1921 debris avalanche is 4 million m^3. The estimated volume of the three mass movements inferred to have come from the cirque--about 85 million m^3—is larger than the volume inferred to have been removed from the cirque. Dilation of the original rock mass and accretion (through inclusion of alluvial, colluvial, and bedrock clasts) could account for the larger volume.

HAZARDS ASSESSMENT

Slope Failure

This study shows that the most catastrophic events that have occurred on the southwest flank of Mount Adams during postglacial time resulted from slope failure of rock weakened by hydrothermal alteration. Landslides of such rock masses disaggregate and move downslope under the influence of gravity, thereby forming lahars and debris avalanches. Slope failure occurs if forces driving failure exceed those resisting failure. Hydrothermal alteration, changes in pore-pressure gradient, erosion of slope support, and fracturing by freezing of ice all decrease slope stability and set the stage for failure. Loading by ice and snow, magmatic eruptions, phreatic explosions, and earthquakes are processes that could increase stress and trigger slope failure. Earthquakes and explosions trigger slope failure when the magnitude of shaking is sufficient to dislodge a mass of rock so that the mass is free to move downslope. Failure, if it occurs, develops along a surface on which shearing stress is greater than shearing strength, and the most likely failure surface is the one on which the ratio of strength to stress is a minimum, called the maximum stressed surface (Spangler and Handy, 1973, p 487). Hydrothermal alteration of the pyroclastic core of Mount Adams has produced zones of weakness within the edifice that increase its susceptibility to slope failure.

Figure 24. Debris flow that occurred, September of 1981, in a tributary of Cascade Creek. Note pack for scale.

Eruptive periods may be separated by hundreds or thousands of years, and hydrothermal alteration may continue between these periods. Reports of sulfurous gases near the summit of Mount Adams throughout historic time (Rusk, 1978, p 257; Fowler, 1935; Phillips, 1941; Hopkins, 1976; Hildreth and others, 1983) and of intermittent steam emissions (Fowler, 1935; Phillips, 1941) suggest continuing hydrothermal alteration at Mount Adams. The presence of hydrothermally altered andesite in the Trout Lake mudflow indicates that alteration processes extend back more than 6,000 years. Prehistoric hydrothermal alteration has variably affected between 0.9 and 3.3 km^3 of rock high on the edifice. Such an immense mass of weakened rock has the potential to produce a mass movement larger than any yet known at Mount Adams.

Clay-sized minerals in hydrothermally altered rock increase porosity but decrease permeability, thereby increasing pore-water capacity of the rock. Moreover, increased hydrothermal activity may melt snow and ice, increasing pore-water content. Increased pore-water content may increase pore-water pressure gradients within the edifice and further weaken the altered rock.

Erosion and weathering processes act to undermine the edifice by removing slope support. Steep slopes, particularly those on the southwest and east sides, are not buttressed well and are thus susceptible to slope failure. Freezing and thawing of water may cause fractures to open that further reduce slope stability. Loading by snow and ice could trigger slope movements on steep slopes, especially those already weakened by hydrothermal alteration; such slope movements could occur without warning.

Shallow earthquakes, explosions, and slope deformation, processes that commonly precede or accompany magmatic eruptions, can trigger failure by increasing stress acting on a slope. Earthquakes triggered catastrophic slope failures and phreatomagmatic eruptions at Bezymianny in 1956 (Gorshkov, 1959) and Mount St. Helens in 1980 (Lipman and Mullineaux, 1981). The May 1980 eruption of Mount St. Helens was preceded by an interval of several months, during which intrusion of magma at a shallow depth caused deformation and abundant shallow earthquakes. Magma could intrude at a shallow depth within the cone of Mt. Adams; however, judging from its past behavior, Mount Adams is not likely to erupt explosively like Mounts St. Helens or Bezymianny. Nevertheless, intrusion of magma within the cone would cause deformation that would fracture and thereby weaken the edifice. Concurrent earthquakes and phreatic explosions could trigger a large landslide. Judging from historical examples, several weeks to several months of precursory activity would probably precede an eruption.

Earthquakes and explosions associated with a magmatic eruption at Fugen- dake of Unzen volcano complex in Japan, triggered a 0.48 km3 landslide at neighboring Mayu-yama in 1792 (Katayama, 1974; Siebert and others, 1987). Ota (1973) suggested that saturation of the cone by hydrothermal waters weakened Mayu-yama, thereby contributing to the landslide. At Mount Adams, earthquakes and explosions accompanying a flank eruption could trigger a landslide on any side of the summit edifice. A massive landslide at Mount Adams like that at Mayu-yama could occur on a side of the mountain opposite to the flank eruption.

Phreatic eruptions and volcanic earthquakes have triggered slope failures at several volcanoes during historic time and could trigger future slope failures at Mount Adams. Sudden phreatic explosions caused a catastrophic failure of 1.5 km^3 at Bandai in 1888 (Moriya, 1980), and of 0.14 km^3 at Papandajan in 1772 (Glicken and others, 1987). A steam explosion like that which Crandell and Fahnestock (1965) suggest triggered the rockfall avalanche of 14 million m^3 at Little Tahoma Peak on Mount Rainier in 1963, may have caused the debris avalanche of 1921 at Mount Adams. Landslides triggered by phreatic eruptions are especially hazardous because they may occur suddenly, with little premonitory activity (Siebert and others, 1987).

The largest magnitude, tectonic earthquakes occurring in western Washington in the past 50 years include the Olympia earthquake (magnitude, 7.1) in 1949, and the Seattle earthquake (magnitude, 6.5) in 1965 (Weaver and Smith, 1983). Earthquakes having magnitudes greater than 3.0 occurred between 1977 and 1981 about 25 km both north and east of Mount Adams. During the past 50 years no recorded earthquakes greater than magnitude 5.0 have occurred in the Mount Adams area. Although an earthquake near Mount Adams having a magnitude greater than 5.0. is of low probability, such an event nevertheless is possible, and could trigger a slope failure without warning.

Hazards

Potentially hazardous events that have occurred in the past 12,000 years at Mount Adams, and are likely to occur in the future, include debris avalanches, lahars, floods, lava flows, and small tephra falls. Unprecedented and thus less likely events include explosive eruptions of pyroclastic flows and widespread tephra falls. Because Mount Adams is situated in wilderness surrounded by the Gifford Pinchot National Forest and Yakima Indian Reservation, only volcanic events large enough to affect areas more than about 20 km distant will threaten nearby communities, although smaller events could endanger people working, camping, or hiking on or near the volcano.

Hazards due to Debris Avalanches, Lahars, and Floods

Debris avalanches are especially hazardous because they move at high velocities, travel great distances, and obliterate everything in their paths. The 1980 debris avalanche of Mount St. Helens moved as fast as 250 km/h and averaged 125 km/h (Voight and others, 1983). Estimated velocities of other debris avalanches include 180 km/h at Tokachi-dake, Japan, 1926 (Murai, 1960), and 130 to 150 km/h, Mount Rainier, 1963 (Crandell and Fahnestock, 1965).

Schuster and Crandell (1984) and Siebert and others (1987) suggest a method whereby the runout of a debris avalanche can be estimated. Scheidegger (1973), in a study of landslides with volumes greater than 1 million m^3, has shown that height-to-length ratio, which approximates the coefficient of friction ($f = H/L$), is inversely proportional to volume (V). Voight and others (1983; 1985) showed that the mobility of volcanic debris avalanches exceeds that of other landslides. Height (H) can be determined by measuring the relief between the top of the potential slide mass and some point in the valley below (Schuster and Crandell, 1984). Runout (L) can be calculated once H and f are known. Schuster and Crandell determined a representative coefficient of friction from 11 selected volcanic debris avalanches: they suggest the use of 0.09 and 0.075 as average and conservative coefficients of friction. Siebert and others (1987) suggest that coefficients of friction range from 0.05 to 0.13 and average 0.09 for debris avalanches having volumes greater than 1 km^3; coefficients range from 0.09 to 0.18 and average 0.13 for debris avalanches having volumes between 0.1 and 1 km^3. The relief between the summit of Mount Adams and Trout Lake, the nearest community to Mount Adams along the White Salmon River, is about 3,140 m. Using H equal to 3,140 m, debris avalanches, which have volumes significantly less than 1 km^3 and coefficients of friction of 0.13 or more, should flow no farther than 24 km and would not affect Trout Lake. Debris avalanches that have volumes of about 1 km^3 or more and coefficients of friction between 0.09 and 0.075, might flow 35 to 42 km and could destroy the community of Trout Lake. If future debris avalanches are, like those of the postglacial time, significantly smaller than 1 km^3, they probably will not reach Trout Lake.

Small lahars like those that have occurred at Mount Adams in postglacial time, would flow greater distances because of their greater mobility, than would debris avalanches of similar volume. Thus, small lahars could easily inundate the Trout Lake lowland. The Trout Lake mudflow and the Salt Creek lahar both have volumes considerably less than 0.1 km^3 and low coefficients of friction (0.06 and 0.09).

Whereas debris avalanches result exclusively from slope failure, lahars can form in several ways. The largest lahars from Mount Adams resulted from slope failures of masses of rock, which probably contained so much water that the moving masses transformed into lahars. These cohesive lahars moved as much as 60 km down valley during the past 6,000 years. The Osceola Mudflow at Mount Rainier, a 5,700-year-old lahar that had a similar origin, flowed more than 100 km from its source (Crandell, 1971). In addition, lahars formed by dewatering of debris avalanche deposits flowed more than 100 km from Mount St. Helens in 1980 (Janda and others, 1981). At Mount Adams, small noncohesive lahars also formed from glacial outburst floods but these were of small volume and limited extent. Future lahars of this type are unlikely to affect communities of the White Salmon River drainage, the nearest being about 25 km distant, but might endanger people near the volcano. None of the postglacial lahars studied at Mount Adams are known to have been caused by magmatic eruptions; nevertheless, the interaction of hot rock with snow and ice during eruptions, particularly those occurring at or near the summit, could cause lahars or floods that might flow tens of kilometers down valley.

Lahars are generally restricted to valley bottoms

but may fill confined valleys to depths of tens of meters, and may run up onto obstacles in their path according to the relation $H = v^2/2g$, where H is height of run up; v is velocity; and g is the gravitational constant. The Salt Creek lahar commonly filled confined reaches of upland valleys to a depth of 50 m and ran up as much as 30 m onto obstacles in its path. A much larger prehistoric mudflow at Mount Rainier, the Osceola Mudflow, filled valleys to depths as great as 150 m (Crandell, 1971).

Lahars are hazardous because they can travel tens of kilometers at high velocities and are capable of destroying almost anything in their path. On steep slopes lahars have been reported to move as much as to 180 km/h, and even on gentle slopes may move at velocities of 20 to 40 km/h (Crandell, 1980). People on foot would be unable to escape such lahars. Burial and the impact from rocks and debris are the chief dangers to human life. A mudflow generated during the eruption of Nevado del Ruiz, Colombia, in 1985 killed about 23,000 people in the city of Armero and virtually leveled the town, leaving only concrete foundations in place. Survivors of that mudflow reported not only being repeatedly sucked under the surface of the mudflow, but also having difficulty breathing when at the surface of the flow because mud blocked breathing passages; most survivors were badly bruised and many suffered broken bones (N. Banks, oral communication, 1987).

The dangers of floods resulting from volcanism are similar to those of floods having other causes. Floods can wash out bridges and erode unprotected natural and artificial embankments, thereby causing structures adjacent to river channels to collapse. Unwary people and livestock trapped in flood waters may drown.

Hazards from Lava Flows

If future lava flows are like previous ones of postglacial time at Mount Adams, they will probably originate from vents on the flanks of the volcano and extend a maximum of about 10 km downslope. Typical lava flows at Mount Adams are 20- to 30-m-thick, blocky, andesite flows of the type that are likely to move only a few meters per hour. People on foot could easily avoid such flows. Nevertheless, hot blocks of rock falling down steep, unstable margins could injure people in areas adjacent to active flow fronts. Lava flows will crush or burn permanent structures in their paths, but because Mount Adams is remote, lava flows are unlikely to reach any communities. Lava flows at Mount Adams might destroy roads, trails, and campgrounds, and could easily start forest fires. Once a lava flow begins, it should be easy to predict its approximate path. Like lava flows of the past, future lava flows at Mount Adams probably won't extend more than about 50 m up on obstacles in their path.

Lava flows originating at or near the summit of Mount Adams might flow more rapidly down the steep flanks of the cone and extend greater distances from their vents than those originating on gentler slopes. However, summit- vent flows are unlikely to extend beyond the apron of the volcano, about 15 km distant; moreover, the flows would move more slowly on gentler slopes.

Hazards from Explosive Eruptions

Because Mount Adams has erupted neither pyroclastic flows nor widespread tephras in postglacial time, it is unlikely to erupt similar products in the foreseeable future, but because of its similarity to Mount Rainier, explosive eruptions--if they were to occur--could be modelled on Holocene eruptions documented by Crandell (1971) and Mullineaux (1974). Eruptions could occur at vents almost anywhere on Mount Adams. Pyroclastic flows would be concentrated in valleys and would be unlikely to move more than about 20 km, an area within Gifford Pinchot National Forest and the Yakima Indian Reservation. If pyroclastic flows occurred above snowline or during winter, snow and ice might be melted by hot rock, producing lahars and floods that might flow many tens of kilometers down valleys. Explosive eruptions also might deposit tephra downwind from the active vent. Because of prevailing westerly winds, tephra would most probably be directed eastward but could be directed to any quarter (Crandell and Mullineaux, 1978; Crandell, 1980). A tephra eruption like Holocene eruptions at Mount Rainier probably would extend no more than about 30 km (Mullineaux, 1974).

Mild Strombolian eruptions produce scoria and spatter cones like the one that forms Red Butte on the north flank of Mount Adams (plate 1). Such eruptions throw hot, pasty lava fragments several hundred meters from the vents and may produce minor tephra beds downwind. Hazard to people from ballistic fragments and tephra probably would be insignificant more than a

few kilometers upwind or a few tens of kilometers downwind from the vent. Such flank vents also may be the source of lava flows.

Hazard Zonation

The boundaries of the hazard zones shown in plates 1 and 2 are arbitrary; hazards do not abruptly change or disappear at these boundaries. Rather, hazards decrease gradually from one hazard zone into the next and diminish gradually beyond the outer boundaries of the zones. Because the size, extent, and nature of the next volcanic eruption cannot be predicted, boundaries shown on plates 1 and 2*B* are estimated. Inasmuch as the degree of risk from volcanic phenomena is gradational, hazard zones delineated in plates 1 and 2 are only guidelines. Because of the inverse relation between the number of events and the distance to which they extend, risk is generally greatest on the slopes of the volcano and diminishes with distance away from the volcano. Furthermore, in the case of flowage phenomena, such as debris avalanches, lahars, and floods, risk diminishes with height above the valley floor.

Lahar Hazard Zones

Mapped Holocene lahars, debris avalanches and lahar hazard zones southwest of Mount Adams are shown in plate 2. Lahar hazard zone MA (plate 2*B*) derives from the composite distribution of Holocene lahars of the southwest flank of Mount Adams (plate 2*A*); it includes areas that might be threatened by future lahars, debris avalanches, and floods similar to those that occurred during the Holocene. Hazard zone MA ends at Northwestern lake, a small reservoir having 2,530,000 m^3 (2,050 acre-feet) of total storage and 1,330,000 m^3 (1,080 acre-feet) of evacuative storage. The extent of lahar hazard zone MB is based on the possible occurrence of a lahar or debris avalanche that is much larger than any that have occurred during postglacial time in the White Salmon River drainage.

The probability of a slope failure at Mount Adams is enhanced because of the estimated 0.9 to 3.3 km^3 of hydrothermally altered rock that forms the summit edifice of Mount Adams. Future eruptions, especially from the summit, would greatly increase the likelihood of a catastrophic slope failure at Mount Adams. Huge debris avalanches and lahars are rare, and the probability of their occurrence at a volcano like Mount Adams is difficult to evaluate. Nevertheless, their potential occurrence merits consideration.

The distribution and possible effects of a huge cohesive lahar or debris avalanche at Mount Adams might be anticipated by comparison with the Hood River lahar (plate 2, hazard zone MB). That lahar originated as a massive debris avalanche at Mount Hood, flowed down the Hood River to its confluence with the Columbia River, crossed it, and flowed as far as 2 km up the White Salmon River (orange arrows, plate 2). Although deposits of the Hood River lahar are not preserved within the Columbia River valley downstream of the White Salmon River, it must have dammed the Columbia River thereby causing flooding many kilometers down the Columbia gorge after the debris dam breached. Similar events have occurred at Mount Rainier during the past 6,000 years where five slope failures having volumes between 50 and 3,000 million m^3 formed lahars that swept as far as 100 km down valleys (Crandell, 1971). Of these, four contained substantial admixtures of hydrothermal clay, and at least three were formed duringperiods of time when eruptions at summit vents also occurred. The Electron Mudflow, which occurred at Mount Rainier about 600 years ago had a volume of 200,000,000 to 300,000,000 m^3 and flowed 60 to 70 km to the Puget Sound lowland. If a lahar as large as the Hood River lahar or Electron Mudflow flowed down the southwest flank of Mount Adams, it would probably extend throughout the White Salmon River valley and down to the Columbia River. Presently, the Columbia River is impounded by Bonneville Dam about 32 km downstream from the mouth of the White Salmon River. Bonneville Reservoir has total storage of 700,000,000 m^3 (565,000 acre-feet) and evacuative storage of 140,000,000 m^3 (115,000 acre-feet). A large lahar entering the Bonneville pool might cause huge waves that would flood areas near Hood River and along the banks of the Columbia River downstream (hazard zone MB). Bonneville Reservoir needs to be drawn down in order to contain the large volume of material that a large lahar might transport into it. An immense lahar like the Osceola Mudflow could fill this reservoir and displace sufficient water to overtop Bonneville Dam even if it were drawn down to its minimum operational level. A lahar as voluminous as the Osceola Mudflow, however, has a large recurrence interval--probably of 10,000 years or more at Mount Rainier. Because Mount Rainier has been more

explosive than Mount Adams in Holocene time, such a huge lahar is considered less likely at Mount Adams. Hazard zone MB is based on the occurrence of a lahar, more modest in size (100,000,000 to 500,000,000 m^3) like the Electron Mudflow, but having a greater likelihood of occurrence.

Lava-flow Hazard Zones

The position of lava-flow hazard zones, LA and LB, which are based on the distribution and extent of postglacial lava flows, are shown in plate 1. Hazard zone LA includes areas that might be affected by lava flows originating at or near the summit of Mount Adams and at flank vents within zone LA. Because no lava flows of postglacial time have reached much higher than 50 m on topographic obstructions, lavas originating from zone LA are unlikely to affect high areas designated zone LB. Areas in zone LB will only be affected by lava flows originating within these areas; however, lava flows having a source within zone LB could flow into zone LA. Cinder cones could form anywhere in zones LA or LB. Tephras derived from eruptions producing cinder cones and lava flows might extend beyond the limits of these zones.

Because no lava flows of postglacial time extended more than 18 km from the summit of Mount Adams, the distal margins of lava-flow hazard zones are shown at this distance. Some Pleistocene flows of the Mount Adams-King Mountain fissure zone did extend beyond the 18 km limit and some originated outside of that limit (fig. 1, plate 1). Because it is impossible to determine where the next eruption of the fissure zone will occur and because of the relative antiquity of past eruptive products, no attempt has been made to define hazard zones around the Mount Adams-King Mountain fissure zone. Should eruptions begin in the fissure zone outside of zones LA and LB, the new vent will probably be located near old vents shown on plate 1. Moreover, once the location of a new vent is known, it should be possible to predict the paths of resulting lava flows.

Mitigation of Hazards

Plans concerning the reaction to, and monitoring of, future eruptions need to be outlined to mitigate the effect of potential volcanic hazards. Land use planning is especially effective in keeping people and their property safe from future volcanic events. Areas most at risk could be zoned to prevent construction of permanent residences. Potential closure zones could be established and emergency evacuation plans made prior to the occurrence of hazardous volcanic events. Geophysical monitoring systems could be installed around Mount Adams to determine the frequency and location of earthquakes, the extent of ground deformation, and the thermal activity that might precede or accompany eruptions. Lahar-detection and -warning devices, suitable for rapid deployment, could be installed.

At the first sign of unrest at Mount Adams, information concerning the nature and degree of risk from volcanic events needs to be publicized. In this way people will understand the nature of the threat and will better understand how to react to that threat. Moreover, people in particularly hazardous areas, such as valley bottoms, will be forewarned of the possible need for rapid evacuation.

Danger from lava flows and cinder cones, the magmatic products most likely at Mount Adams, will probably be restricted to public lands within 18 km of the summit. Such eruptions are likely to be preceded by deformation and seismicity beginning days or weeks before they occur. Local, State, and Federal authorities can restrict access to areas likely to be affected by these events before they occur.

Hazards from lahars extend far beyond the flanks of the volcano and may threaten communities tens of kilometers down valleys. Procedures to cope with the threat of lahars, floods, and debris avalanches might include: (1) a plan for restricting travel in hazardous areas during periods of volcanic unrest, (2) establishment of evacuation plans for areas likely to be threatened, (3) installation of detection and warning systems in critical valleys that could detect hazardous flows at early stages and warn residents of valley floors of the need for immediate evacuation (Crandell, 1971). Because lahars that occur during volcanically quiescent periods may occur without warning, the only practical way to cope with them is to install lahar-warning and -detection devices in valley bottoms. Because of the speed at which lahars move, such devices would only be effective if positioned 10 km or more upstream from population centers.

REFERENCES CITED

Bacon, C.R., 1983, Eruptive history of Mount Mazama and Crater Lake Caldera, Cascade Range, USA: Journal of Volcanology and Geothermal Research, v. 18, p. 57-115.

Beverage, J.P., and Culbertson, J.K., 1964, Hyperconcentrations of suspended sediment: Journal of the Hydraulics Division, Proceedings of the American Society of Civil Engineers, p. 117-128.

Byam, F.M., 1921, The Mount Adams slide of 1921: Mazama, v. 6, no. 2, p. 44-46.

Crandell, D.R., 1969, Surficial geology of Mount Rainier National Park, Washington: U.S. Geological Survey Bulletin 1288, 41 p.

——, 1971, Postglacial lahars from Mount Rainier Volcano, Washington: U.S. Geological Survey Professional Paper 677, 75 p.

——, 1980, Recent eruptive history of Mount Hood, Oregon, and potential hazards from future eruptions: U.S. Geological Survey Bulletin 1492, 81 p.

Crandell, D.R., and Fahnestock, R.K., 1965, Rockfalls and avalanches from Little Tahoma Peak on Mount Rainier, Washington: U.S. Geological Survey Bulletin 1221-A, 30 p.

Crandell, D.R., and Miller R.D., 1974, Quaternary stratigraphy and extent of glaciation in the Mount Rainier region, Washington: U.S. Geological Survey Professional Paper 847, 59 p.

Crandell, D.R., Miller, R.D., Glicken H.X., Christiansen, R.L., and Newhall, C.G., 1984, Catastrophic debris avalanche from ancestral Mount Shasta volcano, California: Geology, v. 12, p. 143-146.

Crandell, D.R., and Mullineaux, D.R., 1973, Pine Creek volcanic assemblage at Mount St. Helens, Washington: U.S. Geological Survey Bulletin 1383-A, 23 p.

——, 1978, Potential hazards from future eruptions of Mount St. Helens Volcano, Washington: U.S. Geological Survey Bulletin 1383-C, 26 p.

Cunningham, C.G., Jr., and Hall, R.B., 1976, Field and laboratory tests for the detection of alunite and determination of atomic percent potassium: Economic Geology, v. 71, p. 1596-1598.

Fisher, R.V., and Schmincke, H.U., 1984, Pyroclastic rocks: Springer-Verlag, Berlin, 472 p.

Fowler, C.S., 1935, The origin of the sulphur deposits of Mount Adams: Pullman, Wash., Washington State University, M.A. thesis, 23 p.

Frank, D.G., 1983, Origin, distribution, and rapid removal of hydrothermally formed clay at Mount Baker, Washington: U.S. Geological Survey Professional Paper 1022-E, 31 p.

——, 1985, Hydrothermal processes at Mount Rainier, Washington: Seattle, Wash., University of Washington, Ph.D. thesis, 195 p.

Glicken, H.X., 1982, Criteria for recognition of large volcanic debris avalanches, *in* EOS: Transactions, American Geophysical Union, v. 63, no. 45, p. 1141.

——, 1986, Rockslide-debris avalanche of May 18, 1980, Mount St. Helens Volcano, Washington: Santa Barbara, Calif., University of California, Ph.D. thesis, 303 p.

Glicken, H.X., Asmoro, P., Lubis, H., Frank, D., and Casadevall, T., 1987, The 1772 debris avalanche and eruption at Papandayan Volcano, Indonesia, and hazards from future eruptions, *in* Hawaii Symposium on how Volcanoes Work: Diamond Jubilee, Hawaiian Volcano Observatory, Hilo, Hawaii, January 19 - 25, 1987, p. 91

Gorshkov, G.S., 1959, Gigantic eruption of the volcano Bezymianny: Bulletin Volcanology, v. 21, p. 77-109.

Hall, R.B., and Bauer, C.W., 1983, Alunite, *in* Lefond, S.J., ed., Industrial Minerals and Rocks, 5th edition: American Institute of Mining Engineers, p. 417-434.

Hammond, P.E., 1980, Reconnaissance geologic map and cross sections of southern Washington Cascade Range; latitude 45°30′ – 47°15′N., longitude 120°45′ – 12°22'.5' W.: Department of Earth Sciences, Portland State University, Portland, Oreg., 2 sheets, 31 p.

Hammond, P.E., Bentley, R.D., Brown, J.C., Ellingson, J.A., Swanson, D.A., 1977, Volcanic stratigraphy and structure of the southern Cascade Range, Washington, *in* Brown, E.H., and Ellis, R.C., eds., Geological Excursions in the Pacific Northwest: Geological Society of America 1977 Annual Meeting, Seattle, p. 127-169.

Hammond, P.E., Pedersen, S.A., Hopkins, K.D., Aiken, Dan, Harle, D.S., Danes, Z.F., Konicek, D.L., and Stricklin, C.R., 1976, Geology and gravimetry of the Quaternary basaltic volcanic field, southern Cascade Range, Washington, *in* Pezzotti, C., ed., Proceedings of the Second United Nations Symposium on the Development and Use of Geothermal Resources, San Francisco, May 20-29: v. 1, p. 397-405.

Hemley, J.J., and Jones, W.R., 1964, Chemical aspects of hydrothermal alteration with emphasis on hydrogen metasomatism: Economic Geology, v. 59, p. 538-569.

Hemley, J.J., Hostetler, P.B., Gude, A.J., and Mountjoy, W.T., 1969, Some stability relations of alunite: Economic Geology, v. 64, no. 6, p. 599-612.

Hildreth, Wes, Fierstein, Judy, 1995, Geologic map of the Mount Adams volcanic field, Cascade Range of Southern Washington: U.S. Geological Survey Miscellaneous Investigations Series Map I-2460, scale 1:50,000.

Hildreth, Wes, Fierstein, Judy, and Miller, M.S., 1983, Mineral and geothermal potential of the Mount Adams Wilderness and contiguous roadless areas, Skamania and Yakima Counties, Washington: U.S. Geological Survey Open-File Report 83-474, 18 p.

Hildreth, Wes, and Lanphere, M.A., 1994, Potassium-argon geochronology of a basalt-andesite-dacite arc system: The

Selected Series of U.S. Geological Survey Publications

Books and Other Publications

Professional Papers report scientific data and interpretations of lasting scientific interest that cover all facets of USGS investigations and research.

Bulletins contain significant data and interpretations that are of lasting scientific interest but are generally more limited in scope or geographic coverage than Professional Papers.

Water-Supply Papers are comprehensive reports that present significant interpretive results of hydrologic investigations of wide interest to professional geologists, hydrologists, and engineers. The series covers investigations in all phases of hydrology, including hydrogeology, availability of water, quality of water, and use of water.

Circulars are reports of programmatic or scientific information of an ephemeral nature; many present important scientific information of wide popular interest. Circulars are distributed at no cost to the public.

Fact Sheets communicate a wide variety of timely information on USGS programs, projects, and research. They commonly address issues of public interest. Fact Sheets generally are two or four pages long and are distributed at no cost to the public.

Reports in the **Digital Data Series (DDS)** distribute large amounts of data through digital media, including compact disc-read-only memory (CD-ROM). They are high-quality, interpretive publications designed as self-contained packages for viewing and interpreting data and typically contain data sets, software to view the data, and explanatory text.

Water-Resources Investigations Reports are papers of an interpretive nature made available to the public outside the formal USGS publications series. Copies are produced on request (unlike formal USGS publications) and are also available for public inspection at depositories indicated in USGS catalogs.

Open-File Reports can consist of basic data, preliminary reports, and a wide range of scientific documents on USGS investigations. Open-File Reports are designed for fast release and are available for public consultation at depositories.

Maps

Geologic Quadrangle Maps (GQ's) are multicolor geologic maps on topographic bases in 7.5- or 15-minute quadrangle formats (scales mainly 1:24,000 or 1:62,500) showing bedrock, surficial, or engineering geology. Maps generally include brief texts; some maps include structure and columnar sections only.

Geophysical Investigations Maps (GP's) are on topographic or planimetric bases at various scales. They show results of geophysical investigations using gravity, magnetic, seismic, or radioactivity surveys, which provide data on subsurface structures that are of economic or geologic significance.

Miscellaneous Investigations Series Maps or **Geologic Investigations Series (I's)** are on planimetric or topographic bases at various scales; they present a wide variety of format and subject matter. The series also incudes 7.5-minute quadrangle photogeologic maps on planimetric bases and planetary maps.

Information Periodicals

Metal Industry Indicators (MII's) is a free monthly newsletter that analyzes and forecasts the economic health of five metal industries with composite leading and coincident indexes: primary metals, steel, copper, primary and secondary aluminum, and aluminum mill products.

Mineral Industry Surveys (MIS's) are free periodic statistical and economic reports designed to provide timely statistical data on production, distribution, stocks, and consumption of significant mineral commodities. The surveys are issued monthly, quarterly, annually, or at other regular intervals, depending on the need for current data. The MIS's are published by commodity as well as by State. A series of international MIS's is also available.

Published on an annual basis, **Mineral Commodity Summaries** is the earliest Government publication to furnish estimates covering nonfuel mineral industry data. Data sheets contain information on the domestic industry structure, Government programs, tariffs, and 5-year salient statistics for more than 90 individual minerals and materials.

The Minerals Yearbook discusses the performance of the worldwide minerals and materials industry during a calendar year, and it provides background information to assist in interpreting that performance. The Minerals Yearbook consists of three volumes. Volume I, Metals and Minerals, contains chapters about virtually all metallic and industrial mineral commodities important to the U.S. economy. Volume II, Area Reports: Domestic, contains a chapter on the minerals industry of each of the 50 States and Puerto Rico and the Administered Islands. Volume III, Area Reports: International, is published as four separate reports. These reports collectively contain the latest available mineral data on more than 190 foreign countries and discuss the importance of minerals to the economies of these nations and the United States.

Permanent Catalogs

"Publications of the U.S. Geological Survey, 1879–1961" and **"Publications of the U.S. Geological Survey, 1962–1970"** are available in paperback book form and as a set of microfiche.

"Publications of the U.S. Geological Survey, 1971–1981" is available in paperback book form (two volumes, publications listing and index) and as a set of microfiche.

Annual supplements for 1982, 1983, 1984, 1985, 1986, and subsequent years are available in paperback book form.